Effect of density changes on tokamak plasma confinement

F. Spineanu[1, a)] and M. Vlad[1]

National Institute of Laser, Plasma and Radiation Physics Bucharest, Romania

(Dated: March 3, 2015)

A change of the particle density (by gas puff, pellets or impurity seeding) during the plasma discharge in tokamak produces a radial current and implicitly a torque and rotation that can modify the state of confinement. After ionization the newly born ions will evolve toward the periodic neoclassical orbits (trapped or circulating) but the first part of their excursion, which precedes the periodicity, is an effective radial current. It is short, spatially finite and unique for each new ion, but multiplied by the rate of ionization and it can produce a substantial total radial current. The associated torque induces rotation which modify the transport processes. We derive the magnitude of the radial current induced by ionization by three methods: the analysis of a simple physical picture, a numerical model and the neoclassical drift-kinetic treatment. The results of the three approaches are in agreement and show that the current can indeed be substantial. Many well known experimental observations can be reconsidered under this perspective. In reactor-grade plasma the confinement can be strongly influenced by adequate particle fuelling.

PACS numbers: 52.55.Fa, 52.20.Dq, 52.25.Fi

[a)] florin.spineanu@euratom.ro

I. INTRODUCTION

Every event of ionization of a neutral particle in tokamak plasma it followed by the displacement of the newly born charges (electron and ion) towards the equilibrium orbits. They leave the magnetic surface where they have been created, due to the neoclassical drift, and evolve towards stationary trajectories. Since the electrons drift much less than the ions, the main effect is associated with the newly born ions. Neglecting collisions, the ions will settle on circulating or trapped orbits and during the periodic motions they depart radially, relative to a certain magnetic surface, alternatively to larger and respectively to smaller radius. Since these positive and negative radial deviations relative to the magnetic surface compensate, the time average shows no effective radial displacement: the orbit has an effective "center" which corresponds to the spatial average of the successive positions of the ion (for example: the "center" of a banana, for the trapped ion; we neglect smaller neoclassical motions of this "center", like the toroidal drift). However there is a part in the radial excursion of the new ion which remains uncompensated. This is precisely the first interval, just after the ionization, when the ion evolves to take the periodic trajectory, and its successive positions do not yet average to the "center". This displacement, from the position where ionization takes place, towards the "center" of the periodic trajectory, is an effective radial current. At the end of this finite, transitory part, the motion becomes periodic and there is no radial current. The radial current of the first part is a source of torque, implicitly rotation and in this way has an impact on the quality of the confinement. It effectively makes a connection between the density change (via pellets, gas puff or impurity seeding) and the change of the confinement. We note that there is a considerable experimental evidence that the variation of density (during the discharge) produces a change in the quality of the confinement.

On a fast time scale a radial electric field is generated by the charge separation: the electrons are almost tied to the magnetic surface, while the ions will travel with the neoclassical drift velocity to their "center", on a distance about half of a banana width. We estimate the radial current and obtain an order of magnitude of the rate of the torque. Compared with the damping rate of a poloidal rotation by transit time magnetic pumping, the ionization-induced rate can be substantially higher. Some improved regimes in JET, as "pellet enhanced performance" (PEP)[1],[2], DIII-D[3],[4] and confinement changes observed in

many devices[5],[6],[7],[8] appear to be connected with this effect of density variation.

The ionization-induced torque has a direction which is fixed by neoclassical orbit's geometry and it interacts with any pre-existing rotation which may have been induced by Reynolds stress, Stringer mechanism or by external factors (NBI, ICRH). The new torque can enhance the pre-existing rotation or can act against it, which makes difficult to predict its consequences in all situations.

We suggest that this process may be a unifying connection between a wide class of regimes where it has been noted a correlation between a dynamic change of density (within a discharge) and the change of the confinement.

According to the preceding explanation, there are two mechanisms that are responsible for this connection

(1) the change of density via ionization (of a pellet, gas puff, impurity seeding or influx of neutral atoms from the edge) means that $\sqrt{\varepsilon}$ ($\varepsilon = r/R$) fraction of the newly created ions are trapped and are moving radially to occupy the positions (the "centers") which are the averages of positions on the trapped (banana) orbits. While after arriving there the bounce averaged radial displacement is zero for the trapped ion, the first step, when the ion moves from the place where it has been created to the "center" of the banana is a net radial current, a single and unrepeatable event for every ionization event. The ensemble of such events is a radial current that produces a torque which generates poloidal rotation and sustains it against magnetic pumping[9]; the sheared poloidal rotation is a barrier that reduce the turbulence and enhances the confinement.

(2) every conversion of a trapped ion into a circulating one (and equally the reversed process), is accompanied by a substantial radial drift. This is because the "centers" of the two kinds of orbits are different and the change from one type of periodic motion (*e.g.* trapped) to the other type of periodic motion (circulating) goes through an intermediate regime, unique and transitory. It consists of the last part of the motion on banana, when the periodicity is lost, followed by the first part of the motion, until the new periodicity is established. Both these parts are unique and transitory and are manifested as a radial current which produces a torque. Then any dynamic process which implies a (slow or fast) change in the velocity space in the region: trapped/circulating ions, will produce a torque. It is interesting to note that this is a mechanism of *direct* coupling between the toroidal and

poloidal rotation. If for some reason a toroidal flow occurs in plasma, a number of trapped ions will have increased their parallel velocity and will change from trapped to circulating[10]. The associated radial current produces a poloidal torque. Conversely, stopping the toroidal rotation leads a subset of the ion population to convert from circulating to trapped, which again produces a transient radial current and further poloidal rotation.

In the present work we concentrate on only the first of the two processes.

Several effects can be connected with this ionization-induced torque. Regimes that are confirmed by experiments, like the mentioned PEP, density peaking and/or anomalous density pinch may have a connection with this torque. The dynamic charge separation that occurs when the ions move from the place of ionization to the "center" of the neoclassical periodic orbit induces a return current of the background ions. Since the number of new ions generated by ionization of a pellet is episodically comparable with the local background ion density, the response motion of this latter population takes the aspect of a massive, even if short, radial displacement. On a relatively large space interval, on which the radial derivative of the rate of ionization [$\partial S/\partial x$ in Eq.(22) below] keeps the same sign, the displacement of the background ions has a unique direction and is sustained all along the total time of ionization. This appears as a density pinch, eventually contributing to the density peaking. Since this equally involves the impurity ions, it can provide a new mechanism for the impurity accumulation.

We note that the ionization of impurity atoms leads to much larger radial drifts and in consequence larger radial currents and torque. This must be examined in relation with impurity (argon) seeding at the edge and with Li pellets in the core. In general any influx of neutral atoms in the plasma will be a source of rotation which affects the local conditions, including the possibility of being a trigger for the L to H mode transition.

We give in the next Sections a simple description of the statistical build-up of a radial current associated with the ionization. At this level of description the collisions are neglected, as are the dispersions of the absolute magnitude of velocities, and of the parallel velocities. The intention is to draw attention to the high amplitude of this current. Further, our result is confirmed by the drift-kinetic neoclassical approach, developed in parallel to the classical treatments of Rosenbluth and Hinton for the similar cases of the torque induced by *alpha* particles[11] and by *neutral beam injection* (NBI)[12].

II. ESTIMATION OF THE RADIAL CURRENT GENERATED AT IONIZATION

A. The contributions to the current

For an easier discussion we adopt a simple picture, mainly having in mind the pellet injection. The source is considered to be limited to a finite segment $[r_1, r_2]$ on the radius r, placed somewhere between $r = 0$ (magnetic axis) and $r = a$ (edge). Due to the symmetry we take the segment as lying in the equatorial plane. The words "left" or "right" refer to this segment, with left being closer to the magnetic axis. The newly born ions will move to place themselves on the periodic neoclassical trajectories, banana or circulating. A radial current is produced during only the first, unique and transitory, part of the trajectory, which is about half of the width of the banana.

We start with a purely geometric example. Consider the motion of a point on a circle C with radius R and center at $(x = R, y = 0)$ on the Ox axis. We introduce the angle $\theta(t)$ between the Ox axis and the radius from the center of the circle $(R, 0)$ to the position of the point on the circle (x, y). θ increases clockwise. The point starts from the origin $(x = 0, y = 0)$, $\theta(t = 0) = 0$. The equations are: $x(t) = R - R\cos[\theta(t)]$ and $y(t) = R\sin[\theta(t)]$. The motion on C is assumed uniform $\theta(t) = \omega t$. The average of the positions of the point $(x(t), y(t))$ up to the current time t are $\overline{x}(t) = \frac{1}{t}\int_0^t dt' x(t') = R - \frac{1}{t}R\frac{1}{\omega}\sin(\omega t)$ with $\overline{x}(t = 0) = 0$ and $\overline{y}(t) = \frac{1}{t}\int_0^t dt' R\sin(\omega t') = \frac{R}{\omega t}[1 - \cos(\omega t)]$, with $\overline{y}(t = 0) = 0$. Clearly the asymptotic $t \to \infty$ average position will be $(R, 0)$, which is the "center" and, after a transient phase, the motion is periodic. The speed with which the average position moves is $d\overline{x}/dt = (R/\omega)\, t^{-2}\sin(\omega t) - Rt^{-1}\cos(\omega t)$. We note that the y-projection of the average, $\overline{y}(t)$, is always positive and that for small time, $t \ll \omega^{-1}$, the x-projected average is linear in time $\overline{x}(t) \approx (R\omega^2/3)\, t$. Both properties will also be found for banana orbits.

The speed of the ions on this transient part of its motion is the neoclassical drift velocity $\mathbf{v}_{Di} = (1/\Omega_{ci})\,\widehat{\mathbf{n}} \times \left(\mu\nabla B + v_\parallel^2\,(\widehat{\mathbf{n}}\cdot\nabla)\,\widehat{\mathbf{n}}\right) \approx \Omega_{ci}^{-1}\left(v_\perp^2/2 + v_\parallel^2\right)/R$. Here Ω_{ci} is the ion cyclotron frequency, $v_{\perp,\parallel}$ are respectively the perpendicular and the parallel velocity of the ion, $\mu = v_\perp^2/(2B)$ is the magnetic moment, $\widehat{\mathbf{n}} = \mathbf{B}/|\mathbf{B}|$ is the versor of the magnetic field $\mathbf{B}$ and R is the radius of curvature of the magnetic line. We introduce the notation v_{Di} , constant and positive. The sign of the velocity will be given according to the particular type

of ion's motion and according to the helical orientation of the magnetic field line. The latter is given by the direction of the plasma current, which we take in the following anti-parallel to the main magnetic field.

We consider first the trapped (t) ions that have, at the moment of ionization, parallel velocity in the same direction with the magnetic field ($+\parallel$) and we note that their banana is entirely outside the magnetic surface on which the ionization has taken place. The ion radial displacement, on the length $d = \Delta^{t+} \approx$ half of the ion banana and only on the time interval of this displacement $\delta t = \Delta^{t+}/v_{Di}$, is toward the edge.

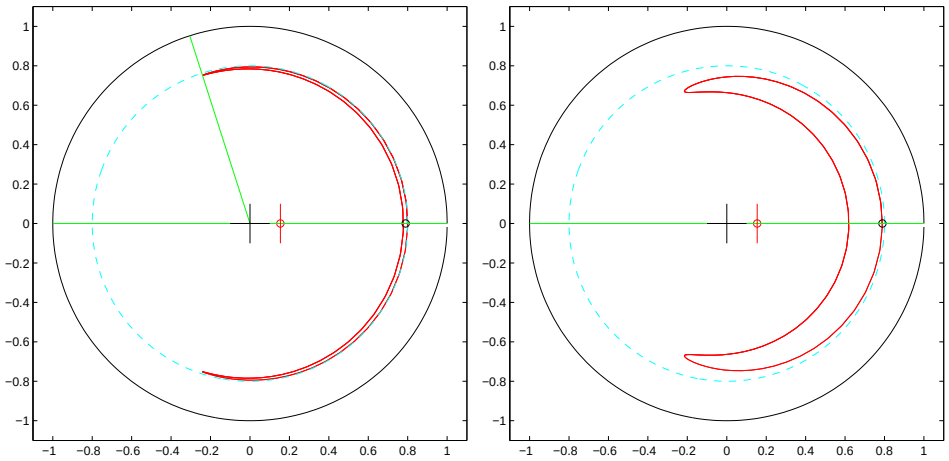

Figure 1: The banana orbit of an ion, which is fully inside the magnetic surface where it has been created. The magnetic surface is represented by the *cyan* dashed circle. The open black dot corresponds to the *center* of the positions $r\,(t)$. The open red dot (and the small red vertical line) indicate the *center* of the positions on the coordinate $x\,(t)$. Just for better visibility we show the orbit dilated along the radius by an arbitrary factor ($\times 10$).

The trapped ions that have in the point of ionization a velocity anti-parallel to the magnetic field vector, ($-\parallel$) have banana orbit entirely inside the magnetic surface and the transitory displacement of the new ion, until the "center" of this banana, is towards smaller r radius, $d = -\Delta^{t-} < 0$ (where Δ^{t-} is defined positive).

In addition there are circulating (c) new ions, *i.e.* on untrapped orbits. Those that have at the initial point a momentum directed parallel to the magnetic field ($+\parallel$) have a circular orbit which is entirely inside the magnetic surface on which the ionization has taken place. The effective displacement to the virtual center is toward larger radius, $d = \Delta^{c+} > 0$ (Δ^{c+} is defined positive).

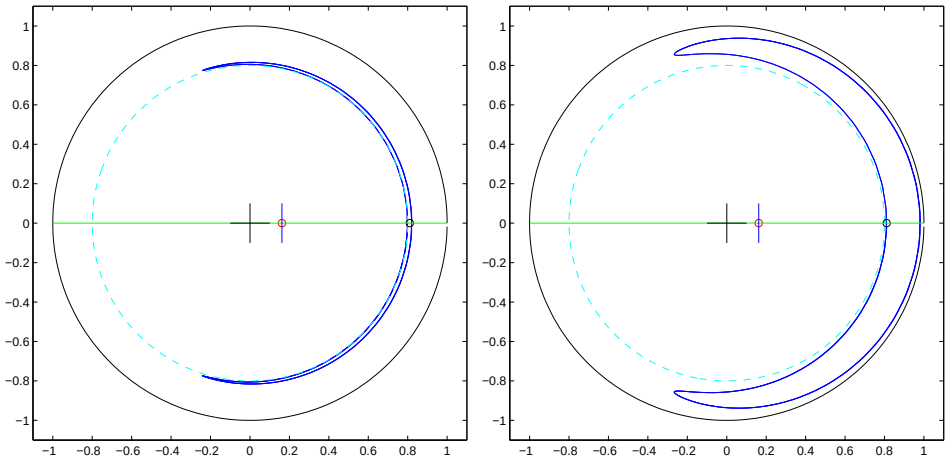

Figure 2: The banana orbit of an ion, which is outside the magnetic surface. The magnetic surface is represented by the *cyan* dashed circle. The open black dot corresponds to the *center* of the positions $r\,(t)$. The open red dot (and the small blue vertical line) indicate the *center* of the positions on the coordinate $x\,(t)$. Just for better visibility we show the orbit dilated along the radius by an arbitrary factor ($\times 10$).

The last type consists of ions that are circulating and with their velocity at the initial point anti-parallel to the magnetic field ($-\,\|$). For them the closed orbit fully includes the magnetic surface and it is equivalent to the displacement of the average position of the new ion to smaller r, toward the magnetic axis, $d = -\Delta^{c-} < 0$ (Δ^{c-} is defined positive).

The four contributions to the current through (r, t), from the two pairs (*i.e.*($\pm\,\|$)-trapped, respectively ($\pm\,\|$)-circulating) appear to be small and they partly compensate, having opposite signs. However, even the small remaining (effective) radial displacement, multiplied with the rate of generation of new ions, leads to a significant radial current. There is another aspect: the centers of the two bananas discussed above [($+\,\|$) and ($-\,\|$)] are spatially separated and we can associate to them the full population of new ions generated in those two positions. The rate of ionization, expressed in number of ions per m^3 per second has a significant radial variation, both for pellets and for gas-puff: the rate of generation of new ions may differ substantially between two radial positions, even if they have small separation, of the order of centimeters. The two banana centers are separated by a distance $\Delta^{t+} + \Delta^{t-}$ which is in this range and suggests that the radial variation of the rate of ionization is an important factor.

For any point r, the four contributions combine into a single, short-lived, finite-spatial

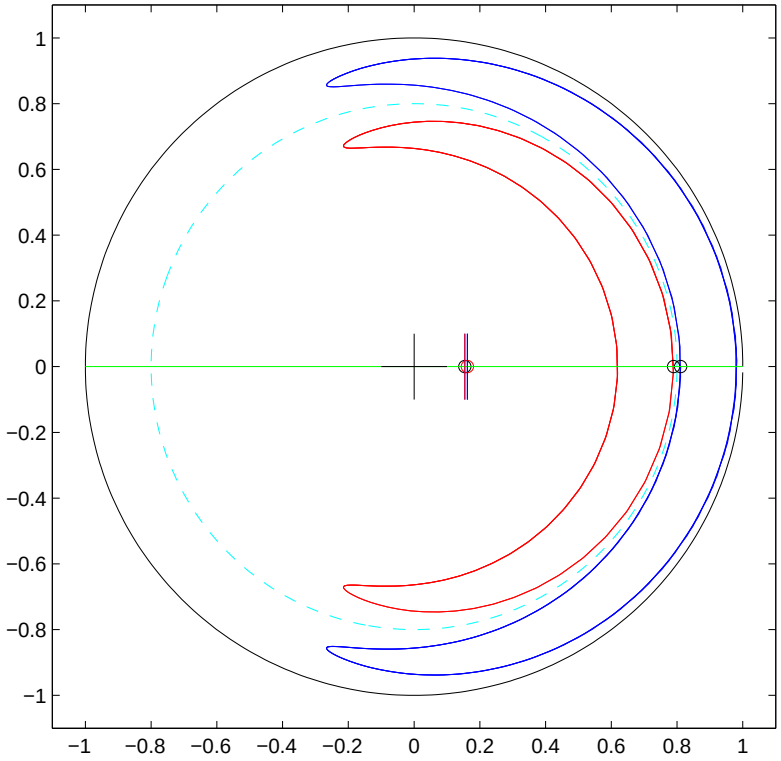

Figure 3: The banana orbits of two ions. One is inside (red) the other is outside (blue) the magnetic surface. The magnetic surface is represented by the *cyan* dashed circle. The two open black dots correspond to the *centers* of the positions $r\,(t)$, for each orbit. The two open red and black dots (and the small red and blue vertical lines) indicate the *centers* of the positions on the coordinates $x\,(t)$ for both orbits. For better visibility we multiply the radius coordinate of each orbit by an arbitrary factor ($\times 10$).

size - event of ion charge displacement, *i.e.* a current. These events occur everywhere within the radial segment of ionization and for all the time when there are still neutral atoms to be ionized.

B. Calculation of the flux of electric charge of the new ions into a point (r, t)

The pellet contains a total number of particles (neutral atoms) N_t and the ionization takes place in the toroidal volume between the surfaces r_1 and r_2, $V_t = 2\pi^2 R\,(r_2^2 - r_1^2)$. The *total* time for ionization of the particles of the pellet is τ^{ioniz}. The rate of generation of ions

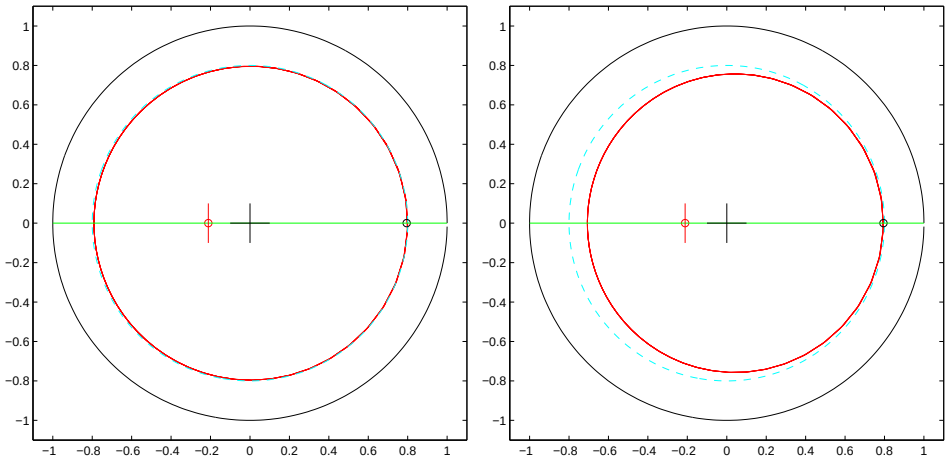

Figure 4: The untrapped (circulating) orbit of an ion, fuly inside the magnetic surface. The magnetic surface is represented by the *cyan* dashed circle. The open black dot corresponds to the *center* of the positions $r\,(t)$. The open red dot (and the small red vertical line) indicate the *center* of the positions on the coordinate $x\,(t)$. Just for better visibility we also show the orbit dilated along the radius by an arbitrary factor ($\times 10$).

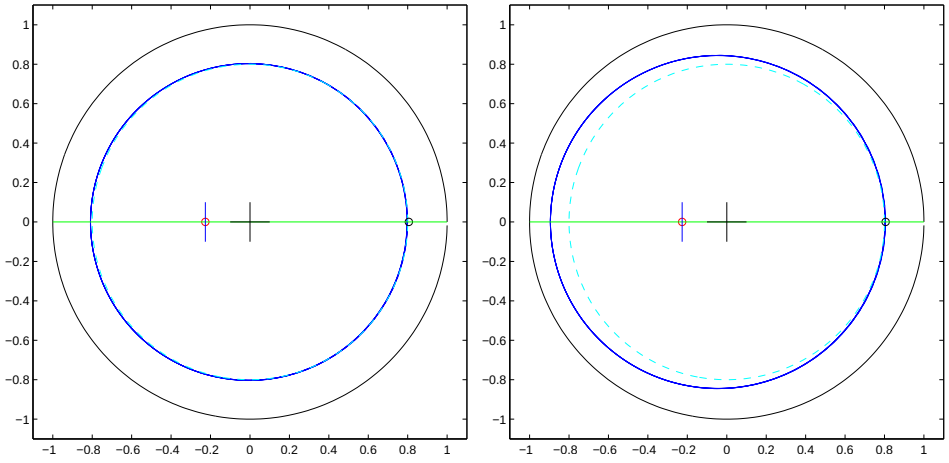

Figure 5: The untrapped (circulating) orbit of an ion, fully outside the magnetic surface. The magnetic surface is represented by the *cyan* dashed circle. The open black dot corresponds to the *center* of the positions $r\,(t)$. The open red dot (and the small red vertical line) indicate the *center* of the positions on the coordinate $x\,(t)$. Just for better visibility we show the orbit dilated along the radius by an arbitrary factor ($\times 10$).

per unit volume and per second has the average magnitude

$$\overset{.}{n}{}^{ioniz}(r,t) \sim \frac{N_t}{\tau^{ioniz}} \frac{1}{V_t} \tag{1}$$

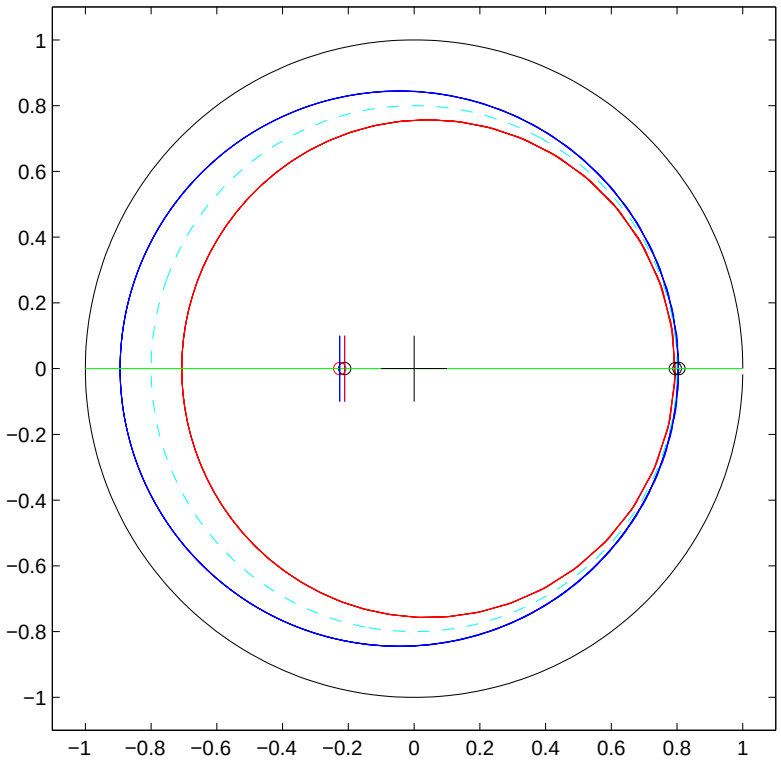

Figure 6: The untrapped (circulating) orbits of two ions fully enclosing (blue) respectively fully inside (red) the magnetic surface. The magnetic surface is represented by the *cyan* dashed circle. The two open black dots correspond to the *centers* of the positions $r(t)$, for each orbit. The two open red and black dots (and the small red and blue vertical lines) indicate the *centers* of the positions on the coordinates $x(t)$ for both orbits. For better visibility we multiply the radius coordinate of each orbit by an arbitrary factor ($\times 10$).

The rate of ionization has strong spatial and temporal variation and we find more convenient to express it as

$$\overset{.}{n}{}^{ioniz}(r,t) = \overset{.}{n}{}_{0}^{ioniz} S(r,t) \left(\frac{ions}{m^3 s}\right) \tag{2}$$

where $S(r,t) \geq 0$ is by definition a nondimensional function representing the space-time variation of the ionization rate. The maximum of S is 1 and its variable is normalized, $x \equiv r/a$. The constant factor $\overset{.}{n}{}_{0}^{ioniz}$ (of order $\sim 10^{23}$ $ions/m^3/s$) is the physical quantity that carries information on the average rate of ionization and is taken from experimental observation. The factors $\overset{.}{n}{}_{0}^{ioniz}$ and S are constraint by the condition

$$\int_0^{\tau^{ioniz}} d\tau \int dV \overset{.}{n}{}^{ioniz}(r,t) = N_t \tag{3}$$

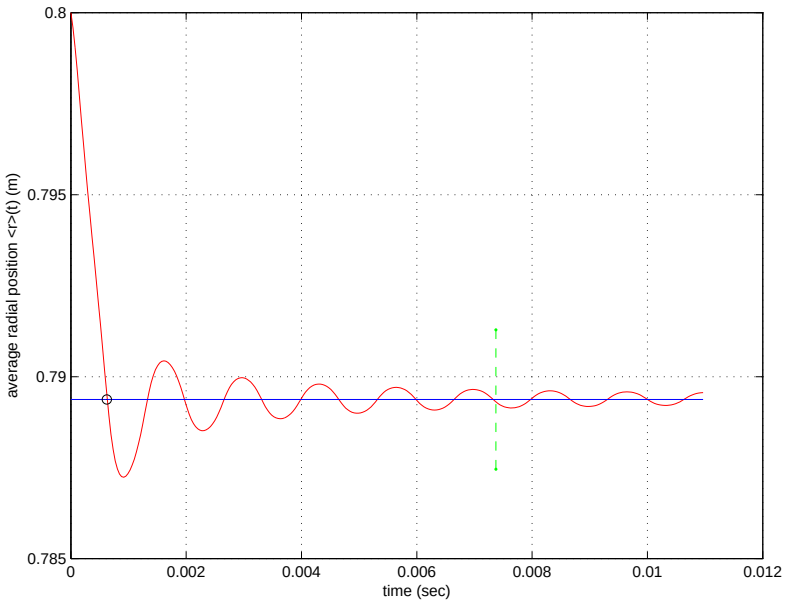

Figure 7: The time evolution of the average radial position $\overline{r}(t)$ for an ions whose orbit is fully inside the magnetic surface. The straight horizontal line is the asymptotic average position r_{asymp} (the "center" of the periodic orbit). The dashed vertical line in the asymptotic range is used to select the part of the trajectory to determine r_{asymp}, far from the transient. The open dot at the intersection of $r = r_{asymp}$ and $r = \overline{r}(t)$ determines the approximative end of the transitory regime, τ_{asymp} . The drift velocity is estimated as $v_{Di} = \frac{r_{asymp} - r_{ini}}{\tau_{asymp}}$, where r_{ini} is the radial position at ionization.

For example, taking for simplicity a source that is constant in time for the entire duration of the ionization $[0, \tau^{ioniz}]$, we have

$$\dot{n}_0^{ioniz} \tau^{ioniz} \int_{r_1}^{r_2} S(r) 4\pi^2 R r dr = N_t \tag{4}$$

The finite volume V_t is divided into toroidal shells of infinitesimal width dr on the minor radius, placed at the position r , with volume $V_{dr} = Adr = 4\pi^2 Rr\,(dr)$ where A is the surface area. We fix a reference position $r \in [r_1, r_2]$, and calculate the net flux of ions that traverses the surface $A = 4\pi^2 Rr$ at r. Consider the bunch of ions that are produced in a time $\delta\tau$, filling the elementary shell (denoted D) situated at a distance ρ from r. Their number is $\dot{n}^{ioniz}\left(r - \rho, t - \frac{\rho}{v_{Di}}\right) \times V_{dr}\delta\tau$. The ions from D that are generated at time $t - \rho/v_{Di}$ travel with constant velocity v_{Di} and arrive in r at time t , traversing the surface A in a time $\delta\tau$. The flux at (r, t), in $(ions/m^2/s)$, is

$$\Gamma(r,t) = \dot{n}^{ioniz}\left(r - \rho, t - \frac{\rho}{v_{Di}}\right) V_{dr}\delta\tau \frac{1}{A}\frac{1}{\delta\tau} = \dot{n}^{ioniz}\left(r - \rho, t - \frac{\rho}{v_{Di}}\right) dr \tag{5}$$

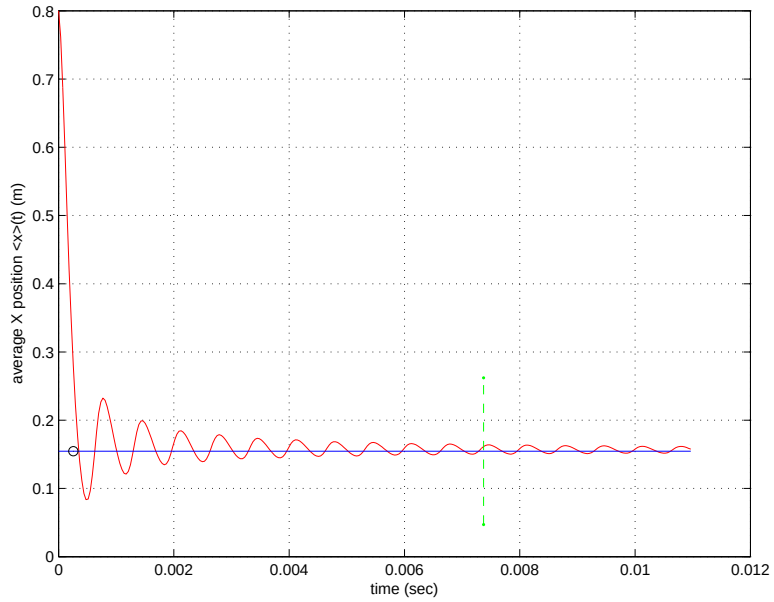

Figure 8: The time evolution of the average x-projection of the position, *i.e.* $\overline{x}\,(t)$, for an ions whose orbit is fully inside the magnetic surface. The details are the same as for Figure 7.

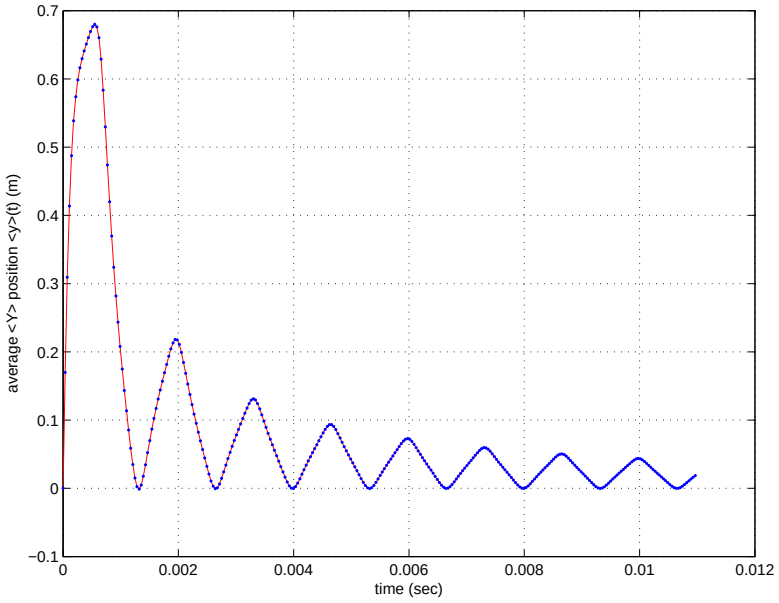

Figure 9: The time evolution of the average y-projection of the position, *i.e.* $\overline{y}\,(t)$, for an ions whose orbit is fully inside the magnetic surface. We note that it remains positive at all times.

The maximum distance of travel on which a new ion generates a current is from the point of ionization until the "center" of the periodic orbit, $\rho_{\max} = \Delta$ (which is one of $\Delta^{t\pm}$). Between $r - \Delta$ and r there are many infinitesimal shells, at distance ρ' from r ($\Delta \geq \rho' \geq 0$). The ions created in these intermediate cells arrive at time t in r if they are generated at $t - \rho'/v_{Di}$.

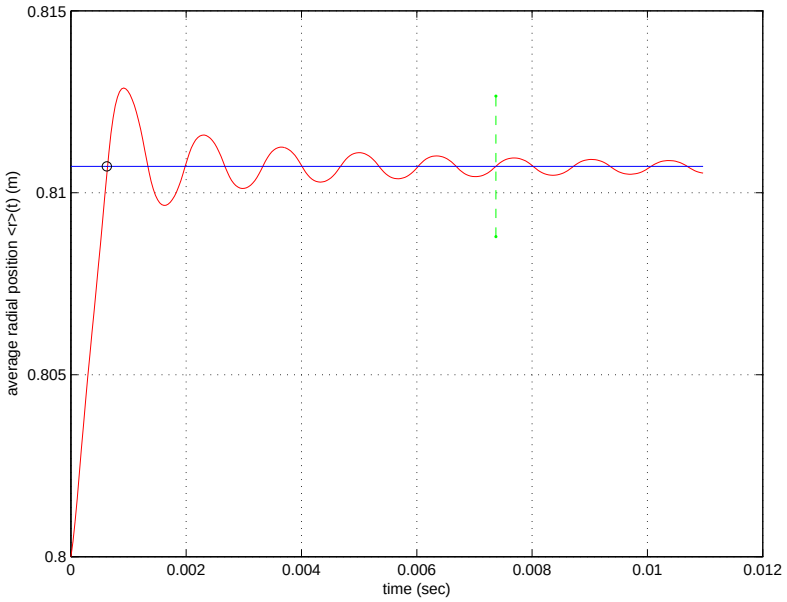

Figure 10: The time evolution of the average radial position $\overline{r}\,(t)$ for an ions whose orbit is outside the magnetic surface. The details are the same as for Figure 7.

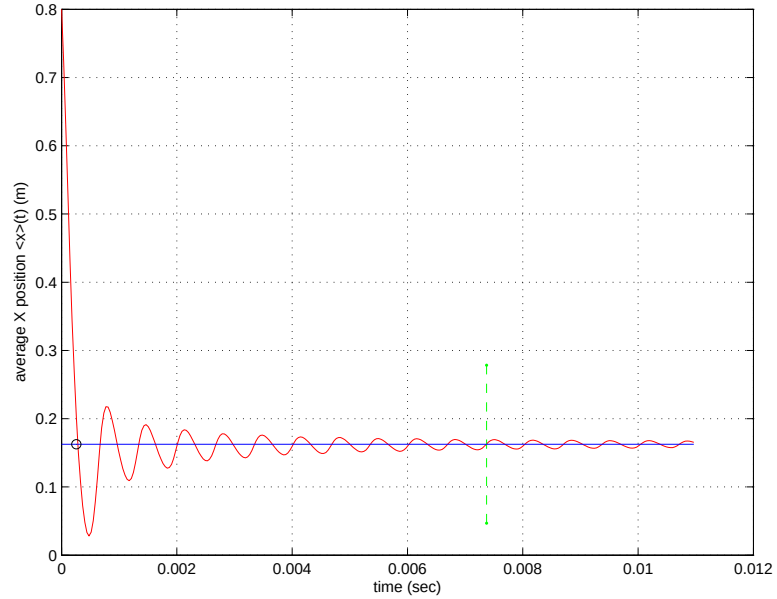

Figure 11: The time evolution of the average x-projection of the position, *i.e.* $\overline{x}\,(t)$, for an ions whose orbit is outside the magnetic surface. The details of the Figure are the same as for Figure 7.

Summing these partial contributions Eq.(5), the origins of which are in the interval $[r-\Delta, r]$

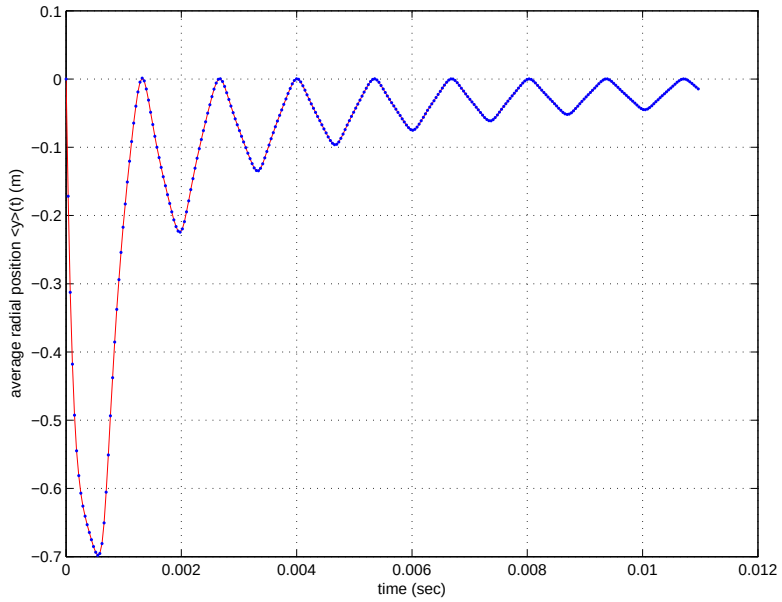

Figure 12: The time evolution of the average y-projection of the position, *i.e.* $\overline{y}\,(t)$, for an ions whose orbit is outside the magnetic surface.

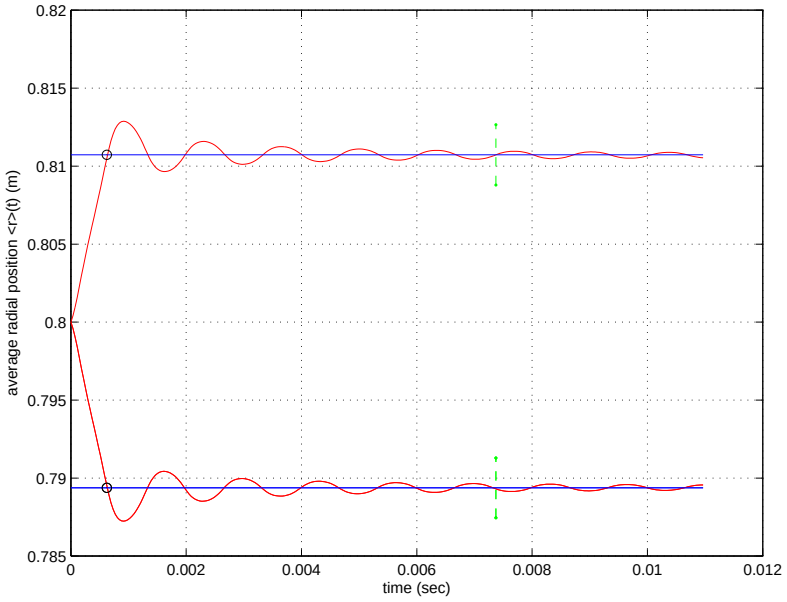

Figure 13: This plot represents the time evolutions of the average positions on r, *i.e.* $\overline{r}\,(t)$, for the trapped particles whose orbits are fully inside (lower curve) and respectively outside (the upper curve) the magnetic surface. The details are the same as in Figure 7.

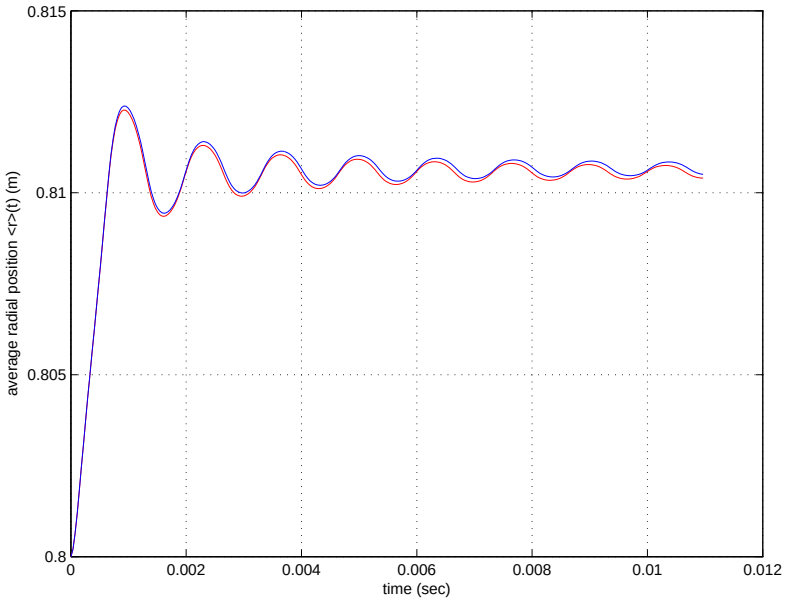

Figure 14: The time variation of the average positions on r, *i.e.* $\overline{r}\,(t)$, for the two types of trapped orbits are represented here with the purpose to give an idea of the smallness of the difference in the average radial displacements. One of the curves (the lower one in Figure 13) has been reversed in order to make easier the comparison.

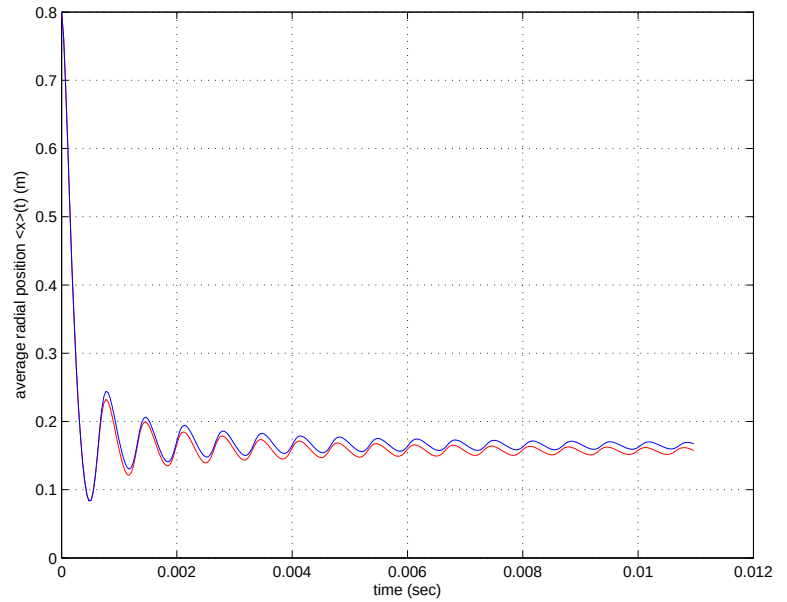

Figure 15: The same as Figure 14 but for the x-projection.

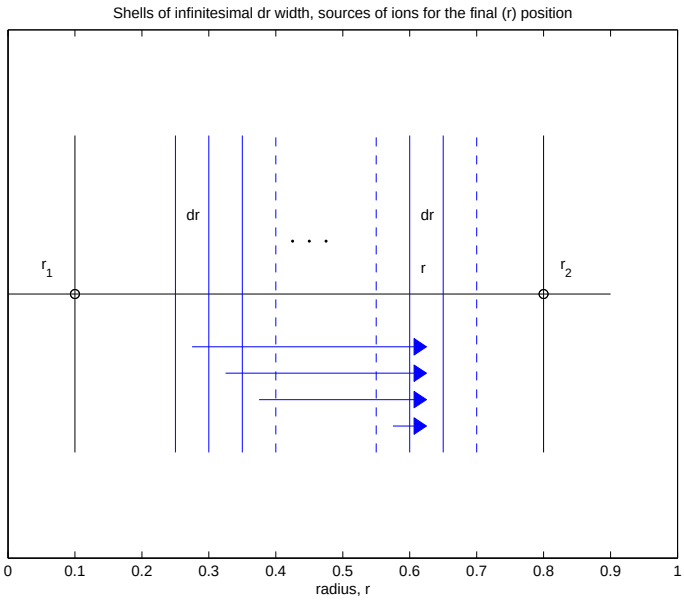

Figure 16: A simple representation of the fluxes that are traversing the surface placed at the radius r, coming from various infinitesimal regions δr. The sum over these contributions is the integral that defines the current density in (r,t) acoording to the text. The positions r_1 and r_2 are the limits of the domain of ionization.

it results $\Gamma^{\Delta}(r,t)$

$$\begin{aligned}\Gamma^{\Delta}(r,t) &= \int_0^{\Delta} \overset{.}{n}^{ioniz}\left(r-\rho',t-\frac{\rho'}{v_{Di}}\right)d\rho' \\ &\approx \overset{.}{n}_0^{ioniz}\int_0^{\Delta} d\rho'\left[S(x,t)-\left(\frac{\partial S}{\partial r}\right)\rho'-\left(\frac{\partial S}{\partial t}\right)\frac{\rho'}{v_{Di}}\right] \\ &= \overset{.}{n}_0^{ioniz}\left[S(r,t)\,\Delta-\frac{1}{2}\left(\frac{\partial S}{\partial r}\right)\Delta^2-\frac{1}{2}\left(\frac{\partial S}{\partial t}\right)\frac{\Delta^2}{v_{Di}}\right]\end{aligned} \tag{6}$$

where the derivatives of S are calculated in (r,t). This flux must be multiplied with the fractional number representing how many of the new ions will settle on trapped, respectively circulating orbits. We take the approximative values $\sqrt{\varepsilon}$ and respectively $1-\sqrt{\varepsilon}$. In addition, we assume that a fraction of $1/2$ new ions have parallel, respectively anti-parallel initial velocities.

C. The current density in (r,t)

Taking into account the four type of ion's orbits, we use Eq.(6) to estimate the flows of new ions coming in, or leaving, the point (r,t). The contributions from neighbor points are

$$\Gamma_{in}^{t(+\|)}(r,t) = \frac{1}{2}\sqrt{\varepsilon}\int_0^{\Delta^{t+}} \overset{.}{n}^{ioniz}\left(r-\rho', t-\frac{\rho'}{v_{di}}\right)d\rho' \tag{7}$$
$$= \frac{1}{2}\sqrt{\varepsilon}\overset{.}{n}_0^{ioniz}\left[S(r,t)\,\Delta^{t+} - \frac{1}{2}\left(\frac{\partial S}{\partial r}\right)\left(\Delta^{t+}\right)^2 - \frac{1}{2}\left(\frac{\partial S}{\partial t}\right)\frac{\left(\Delta^{t+}\right)^2}{v_{Di}}\right]$$

This is the number of ions that are trapped and had an initial velocity parallel with **B**. They are produced in $\left(r-\rho', t-\frac{\rho'}{v_{Di}}\right)$, summed over $[r-\Delta^{t+}, r]$, and flow toward (r,t) from the left (*i.e.* their current is positive).

$$\Gamma_{in}^{t(-\|)}(r,t) = \frac{1}{2}\sqrt{\varepsilon}\int_0^{\Delta^{t-}} \overset{.}{n}^{ioniz}\left(r+\rho', t-\frac{\rho'}{v_{di}}\right)d\rho' \tag{8}$$
$$= \frac{1}{2}\sqrt{\varepsilon}\overset{.}{n}_0^{ioniz}\left[S(r,t)\,\Delta^{t-} + \frac{1}{2}\left(\frac{\partial S}{\partial r}\right)\left(\Delta^{t-}\right)^2 - \frac{1}{2}\left(\frac{\partial S}{\partial t}\right)\frac{\left(\Delta^{t-}\right)^2}{v_{Di}}\right]$$

This is the number of ions that are trapped and had an initial velocity anti-parallel to **B**. They are produced in $\left(r+\rho', t-\frac{\rho'}{v_{Di}}\right)$, summed over the interval $[r, r+\Delta^{t-}]$ and flow towards (r,t) from the right (*i.e.* their current is negative).

$$\Gamma_{in}^{c(+\|)}(r,t) = \frac{1}{2}\left(1-\sqrt{\varepsilon}\right)\int_0^{\Delta^{c+}} \overset{.}{n}^{ioniz}\left(r-\rho', t-\frac{\rho'}{v_{di}}\right)d\rho' \tag{9}$$
$$= \frac{1}{2}\left(1-\sqrt{\varepsilon}\right)\overset{.}{n}_0^{ioniz}\left[S(r,t)\,\Delta^{c+} - \frac{1}{2}\left(\frac{\partial S}{\partial r}\right)\left(\Delta^{c+}\right)^2 - \frac{1}{2}\left(\frac{\partial S}{\partial t}\right)\frac{\left(\Delta^{c+}\right)^2}{v_{Di}}\right]$$

This is the number of ions that are circulating and had an initial velocity parallel with **B**. They are produced in $\left(r-\rho', t-\frac{\rho'}{v_{Di}}\right)$, summed over the interval $[r-\Delta^{c+}, r]$ and flow towards (r,t) from the left (*i.e.* their current is positive).

$$\Gamma_{in}^{c(-\|)}(r,t) = \frac{1}{2}\left(1-\sqrt{\varepsilon}\right)\int_0^{\Delta^{c-}} \overset{.}{n}^{ioniz}\left(r+\rho', t-\frac{\rho'}{v_{di}}\right)d\rho' \tag{10}$$
$$= \frac{1}{2}\left(1-\sqrt{\varepsilon}\right)\overset{.}{n}_0^{ioniz}\left[S(r,t)\,\Delta^{c-} + \frac{1}{2}\left(\frac{\partial S}{\partial r}\right)\left(\Delta^{c-}\right)^2 - \frac{1}{2}\left(\frac{\partial S}{\partial t}\right)\frac{\left(\Delta^{c-}\right)^2}{v_{Di}}\right]$$

This is the number of ions that are circulating and had an initial velocity anti-parallel to **B**. They are produced in $\left(x+\rho', t-\frac{\rho'}{v_{Di}}\right)$, summed over $[r, r+\Delta^{c-}]$ and flow towards (r,t) from the right (*i.e.* their current is negative).

The current density resulting from the *in* fluxes is

$$J^{in}(x,t) = |e|\left(\Gamma_{in}^{t(+\|)} - \Gamma_{in}^{t(-\|)} + \Gamma_{in}^{c(+\|)} - \Gamma_{in}^{c(-\|)}\right) \tag{11}$$

or

$$\begin{aligned} & J^{in}(x,t) \\ &= \frac{1}{2}|e|\dot{n}_0^{ioniz}\left\{S(x,t)\left[\sqrt{\varepsilon}\Delta^{t+} - \sqrt{\varepsilon}\Delta^{t-} + \left(1-\sqrt{\varepsilon}\right)\Delta^{c+} - \left(1-\sqrt{\varepsilon}\right)\Delta^{c-}\right]\right. \\ &\quad + \frac{1}{2}\left(\frac{\partial S}{\partial r}\right)\left[-\sqrt{\varepsilon}\left(\Delta^{t+}\right)^2 - \sqrt{\varepsilon}\left(\Delta^{t-}\right)^2 - \left(1-\sqrt{\varepsilon}\right)\left(\Delta^{c+}\right)^2 - \left(1-\sqrt{\varepsilon}\right)\left(\Delta^{c-}\right)^2\right] \\ &\quad \left. + \frac{1}{2}\frac{1}{v_{Di}}\left(\frac{\partial S}{\partial t}\right)\left[-\sqrt{\varepsilon}\left(\Delta^{t+}\right)^2 + \sqrt{\varepsilon}\left(\Delta^{t-}\right)^2 - \left(1-\sqrt{\varepsilon}\right)\left(\Delta^{c+}\right)^2 + \left(1-\sqrt{\varepsilon}\right)\left(\Delta^{c-}\right)^2\right]\right\} \end{aligned} \tag{12}$$

We now have to calculate the flows (*out*) that leave the shell of the point (r,t).The groups that are leaving (r,t) are:

Trapped with parallel (*i.e.* positive) initial velocity $t(+\|)$

$$n_{out}^{t(+\|)}(r,t) = \frac{1}{2}\sqrt{\varepsilon}\dot{n}^{ioniz}(r,t) \quad \text{(toward large } r\text{)} \tag{13}$$

The second group consists of trapped with anti-parallel (*i.e.* negative) initial velocity

$$n_{out}^{t(-\|)}(r,t) = \frac{1}{2}\sqrt{\varepsilon}\dot{n}^{ioniz}(r,t) \quad \text{(toward small } r\text{)} \tag{14}$$

The third group consists of circulating ions with parallel initial velocity

$$n_{out}^{c(+\|)}(r,t) = \frac{1}{2}\left(1-\sqrt{\varepsilon}\right)\dot{n}^{ioniz}(r,t) \quad \text{(toward large } r\text{)} \tag{15}$$

The fourth group consists of circulating ions with anti-parallel initial velocity

$$n_{out}^{c(-\|)}(r,t) = \frac{1}{2}\left(1-\sqrt{\varepsilon}\right)\dot{n}^{ioniz}(r,t) \quad \text{(toward small } r\text{)} \tag{16}$$

Summing the *out* components after taking into account the signs according to the description

$$J^{out}(r,t) = |e|\left(\Gamma_{out}^{t(\|)} - \Gamma_{out}^{t(-\|)} + \Gamma_{out}^{c(\|)} - \Gamma_{out}^{c(-\|)}\right) = 0 \tag{17}$$

Adding the flows *in* and *out* $J(r,t) = J^{in}(r,t) - J^{out}(r,t)$ we obtain

$$\begin{aligned} & J(r,t) \\ &= \frac{1}{2}|e|\dot{n}_0^{ioniz}\left\{S(r,t)\left[\sqrt{\varepsilon}\left(\Delta^{t+} - \Delta^{t-}\right) + \left(1-\sqrt{\varepsilon}\right)\left(\Delta^{c+} - \Delta^{c-}\right)\right]\right. \\ &\quad + \frac{1}{2}\left(\frac{\partial S}{\partial r}\right)\left[-\sqrt{\varepsilon}\left(\left(\Delta^{t+}\right)^2 + \left(\Delta^{t-}\right)^2\right) - \left(1-\sqrt{\varepsilon}\right)\left(\left(\Delta^{c+}\right)^2 + \left(\Delta^{c-}\right)^2\right)\right] \\ &\quad \left. + \frac{1}{2}\frac{1}{v_{Di}}\left(\frac{\partial S}{\partial t}\right)\left[\sqrt{\varepsilon}\left(-\left(\Delta^{t+}\right)^2 + \left(\Delta^{t-}\right)^2\right) + \left(1-\sqrt{\varepsilon}\right)\left(-\left(\Delta^{c+}\right)^2 + \left(\Delta^{c-}\right)^2\right)\right]\right\} \end{aligned} \tag{18}$$

We show in **Appendix A** that the contributions of the circulating ions is much smaller than that of the trapped ions and for the present estimation can be neglected

$$J(r,t) \approx \frac{1}{2}|e|\,\dot{n}_0^{ioniz}\left\{S(x,t)\sqrt{\varepsilon}\left[\Delta^{t+}-\Delta^{t-}\right]\right. \\ -\frac{1}{2}\left(\frac{\partial S}{\partial r}\right)\sqrt{\varepsilon}\left[\left(\Delta^{t+}\right)^2+\left(\Delta^{t-}\right)^2\right] \\ \left.+\frac{1}{2}\frac{1}{v_{Di}}\left(\frac{\partial S}{\partial t}\right)\sqrt{\varepsilon}\left[-\left(\Delta^{t+}\right)^2+\left(\Delta^{t-}\right)^2\right]\right\} \tag{19}$$

In the numerical model (next Section) we take a time-independent source, $\partial S/\partial t = 0$, and the current density becomes

$$J(r) \approx \frac{1}{2}|e|\,\dot{n}_0^{ioniz}\sqrt{\varepsilon}\left\{S(r,t)\left(\Delta^{t+}-\Delta^{t-}\right)-\frac{1}{2}\left(\frac{\partial S}{\partial r}\right)\left[\left(\Delta^{t+}\right)^2+\left(\Delta^{t-}\right)^2\right]\right\} \tag{20}$$

The distance $\Delta^{t\pm}$ travelled by the new ion from ionization to the "center" of the periodic motion (*i.e.* the distance on which there is effective current) will be calculated in the next Section by solving the equations of motion of the ion, as initial value problem. For the present estimation we adopt neoclassical approximations[13] replacing $\Delta^{t\pm}$ with the "radius" of the banana,

$$\Delta^{\pm} \approx v_{Di}\tau_{bounce} = \rho_i q \varepsilon^{-1/2} \tag{21}$$

where ions $v_{Di} \approx \frac{1}{\Omega_{ci}}\frac{v_{th,i}^2}{R}$ and $\tau_{bounce} \approx r/v_\theta = \frac{rB}{B_\theta}\frac{1}{v_{th,i}}\sqrt{\frac{R}{r}}$[14]. In regions where the ionization rate has strong spatial variation, the second term in Eq.(20) is large and we can simplify the result as

$$J \approx -\frac{1}{2}|e|\,\dot{n}_0^{ioniz}\left(\frac{\partial S}{\partial r}\right)\rho_i^2 q^2 \varepsilon^{-1/2} \tag{22}$$

For an estimation we take $a = 1\ (m)$, $R = 3.5\ (m)$, $B_T = 3.5\,(T)$, $T_i = 1.5\ (keV)$, $N_t = 3\times 10^{21}$ neutral atoms in the pellet, $\tau^{ioniz} \approx 4\times 10^{-3}\ (s)$ duration of the complete ionization process[4],[15] and the radial extension of the zone of ionization is between $r_1 = 0.4a$ and $r_2 = 0.7a$. The energy of the new ions is a fraction ($\eta = 0.75$) of the background ion energy and the trapping parameter $\lambda = hv_\perp^2/v^2$, $h = 1+\varepsilon\cos\theta$ is taken $\lambda = 0.92$. It results $V_t \approx 22.8\ (m^3)$, $A(r) \approx 138r\ (m^2)$ and the average rate of ionization $\dot{n}^{ioniz} \sim 3.3\times 10^{22}\ (ions/m^3/s)$. Adopting for $S(r)$ a simple spatial profile limited between $r_a = 0.475a$, $r_b = 0.625a$, with $\max S = 1$ we find from the constraint Eq.(4) $\dot{n}_0^{ioniz} \approx 1.2\times 10^{23}$ $(ions/m^3/s)$. Using values suggested by experiments[15],[16],[17],[18],[4], $\Delta^{t\pm}$ from exact integration, and $a^{-1}\partial S/\partial x \sim 20\ (m^{-1})$, we obtain from Eq.(20) $|J| \sim 11.52\ (A/m^2)$.

The result is indeed high. For comparison we consider $nm_i\partial v_\theta/\partial t \sim JB_T$. This means $\partial v_\theta/\partial t \sim 23\times 10^8\ \ (m/s^2)$, or, in every microsecond the poloidal speed would increase with more than 4 (km/s). In less than one tenth of a milliseconds v_θ rises to the range of the ion thermal speed $v_{th,i} \sim 0.38\times 10^3\ \ (km/s)$. For comparison the transit time magnetic pumping decay of the poloidal velocity would contribute with

$$-\gamma^{MP} = \frac{\partial}{\partial t}\ln v_\theta = \frac{3}{4}\left(1+\frac{1}{2q^2}\right)\left(\frac{l}{qR}\right)^2 \nu_{ii} \tag{23}$$

where l is the mean free path and ν_{ii} is the ion-ion collision time[19]. We find $-\gamma^{MP} \sim 1.2\times 10^4\ \ (s^{-1})$, and taking a poloidal velocity (as observed in some experiments, *e.g.*[20]) $v_\theta \sim 10^4\ \ (m/s)$ it is estimated $\left|(\partial v_\theta/\partial t)^{MP}\right| \sim 1.2\times 10^8\ \ (m/s^2)$. It results

$$\left(\frac{\partial v_\theta}{\partial t}\right)^{ioniz} > \left|\left(\frac{\partial v_\theta}{\partial t}\right)^{MP}\right| \tag{24}$$

Of course, this ionization torque acts for short time (few milliseconds) and Eq.(22) is an overestimation as long as the neutral atoms' dynamics (*e.g.* the pellet cloud) and the bulk ion's reaction (return current) are not described in detail. But this result is a strong suggestion that the ionization torque is important.

III. NUMERICAL IMPLEMENTATION

The numerical simulation of this process has been done on a discrete mesh $\{r_i\}_{i=1,NX}\times\{t_k\}_{k=1,NT}$ for $NR = NT = 500$. The simple physical picture described above has been implemented.. For any cell (r_i, t_k) we calculate the number of ions that are generated, $\dot{n}_0^{ioniz} S(r,t)$, using the expression for $S(r) = \alpha + \beta(r/a) + \gamma(r/a)^2$. Imposing $S(r_a) = S(r_b) = 0$ and $\max S = 1$ at $(r_a + r_b)/2$, the coefficients are determined and, as explained above, Eq.(4) determines the constant $\dot{n}_0^{ioniz} = 1.2\times 10^{23}\ \ (ions/m^3/s)$. We now assume that the energy of the new ions is a fraction (0.75) of the background ion thermal energy (at $T_i = 1.5keV$) and that the probability of being trapped is $\sqrt{\varepsilon}$. Finally we assume that the probability that the ion has an initial velocity which is parallel to $\mathbf{B}$ is 1/2, equal with the probability to be anti-parallel. Now we look at the way the ions move. The total excursion on r is Δ^{t+} (to larger r) and Δ^{t-} (to smaller r). The displacement is represented on the mesh $\{r_{i'}, t_{k'}\}$ and every cell (i', k') which is traversed by the flux of ions stores

this contribution, adding it to a variable that will finally be the current flowing through it. There are several other cells whose new ions traverse this cell (i', k') and all contributions are counted and summed. Due to the assumed constancy of v_{Di}, there is no decay along the path that starts from (r_i, t_k) and ends in the cell $(r_i + \Delta^{t+}, t + \Delta^{t+}/v_{Di})$, [respectively $(r_i - \Delta^{t-}, t + \Delta^{t-}/v_{Di})$ for the anti-parallel initial velocity]. All cells traversed along this path retain the contribution from (r_i, t_k).

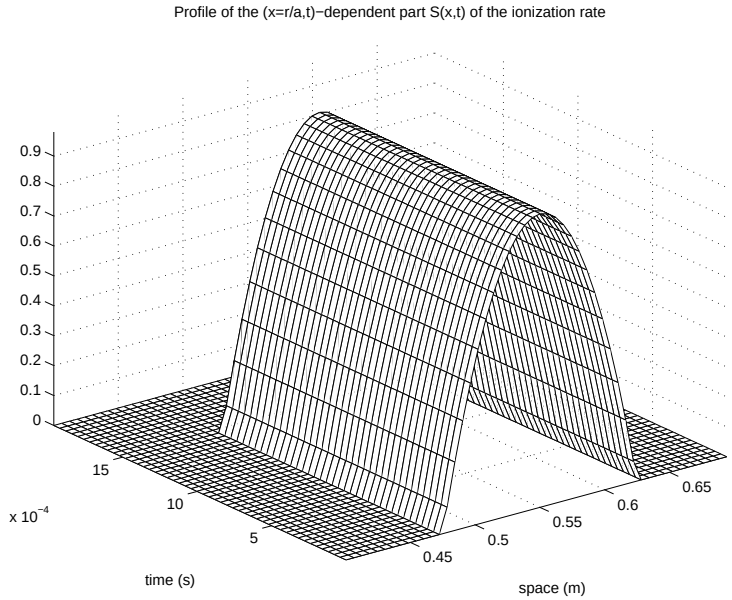

Figure 17: The space-time profile of the ionization source, the function $S(r,t)$. The factor $\dot{n_0}\left(ions/m^3/s\right)$ multiplies this function to obtain the effective rate of production of new ions.

Instead of the neoclassical approximations for $\Delta^{t\pm}$ and v_{Di}[14] we choose to solve the system of equations of motion[21],[22],[23],[24],[13] in every cell $(r_i, t_k)_{i=1,NX;k=1,NT}$.

$$\frac{dr}{dt} \approx -\frac{1}{\Omega}\left(\frac{v_\perp^2}{2} + v_\parallel^2\right)\frac{\sin\theta}{R_0}$$

$$\frac{d\theta}{dt} \approx \frac{v_\parallel}{qR_0} - \frac{1}{r}\frac{1}{\Omega}\left(\frac{v_\perp^2}{2} + v_\parallel^2\right)\frac{\cos\theta}{R_0}$$

$$\frac{d\varphi}{dt} \approx \frac{v_\parallel}{R_0}$$

$$\frac{d}{dt}\left(\frac{v_\perp^2}{2}\right) = \left(\frac{v_\perp^2}{2}\right) v_\parallel \frac{B_\theta}{B_T}\frac{\sin\theta}{R_0}$$

$$\frac{dv_\parallel}{dt} = -\left(\frac{v_\perp^2}{2}\right)\frac{B_\theta}{B_T}\frac{\sin\theta}{R_0}$$

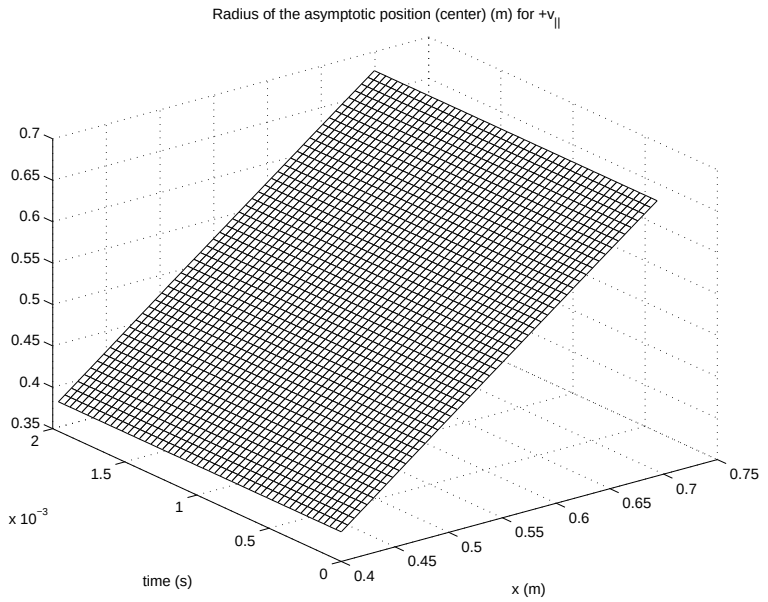

Figure 18: The (r,t) profile of the final position (the "center") of the average $r\,(t)$ for the ions whose orbit encloses the magnetic surface. This is calculated by solving in every (r_i,t_k), for $i=1,NR$, $k=1,NTIME$ cell of the disctere mesh, the set of equations of motion for a trapped ion.

From the solution we get the exact orbit of an ion born in the cell $(r_i,t_k)_{i=1,NR;k=1,NT}$ but we still have to operate the separation of the transitory part, the part which represents the unique manifestation of a current, from the periodic part of the trajectory, whose average does not produce a current. We calculate for each trajectory the time-dependent average position $\overline{r}\,(t)=\frac{1}{t}\int_0^t r\,(t')\,dt'$ and leave the integration sufficiently long such that the asymptotic quasi-static average position $r_{asymp}=\overline{r}\,(t\to\infty)$ to be clearly identified. This position r_{asymp} (the "center" of the banana) is retained and the quantity Δ^t is obtained as the difference between r_{asymp} and the initial position, which is the point of the ionization, r_{ini}. We still need the estimation of the *effective* time that is necessary for the ion to reach this asymptotic position. The first intersection between the asymptotic line $r=r_{asymp}$ and the evolution line $\overline{r}\,(t)$ takes place at a moment t_{asymp}, which is retained as the representative time of ion's travel to the center. This procedure is admittedly approximative but we have tried several reasonably alternative methods and the present one seems the best.

Once we know $r_{asymp}-r_{ini}\equiv\Delta$ and t_{asymp} we find $v_{Di}=\Delta/t_{asymp}$ and all data for the displacements of the new ions originating from (r_i,t_k) on the mesh are now available. In every cell the system is solved for both parallel and anti-parallel initial velocities and

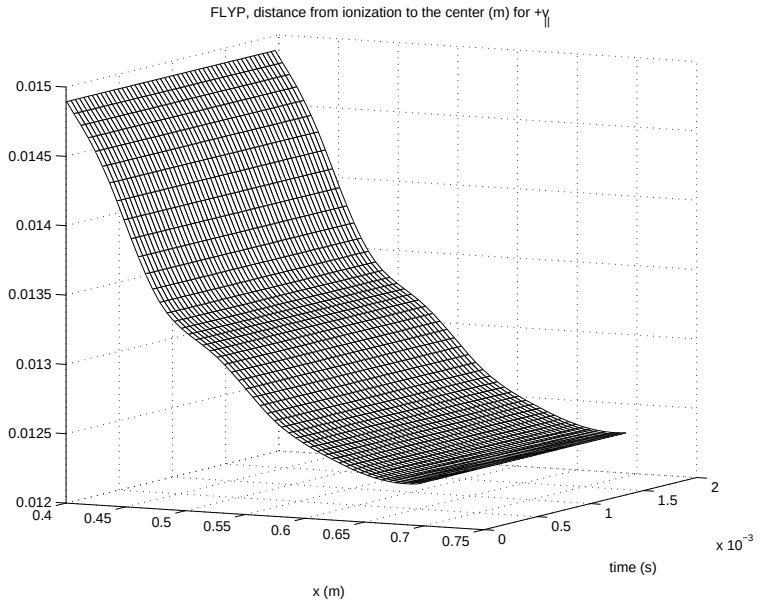

Figure 19: The variable $FLYP$, difference between the final position (the "center" of the banana) and the initial radial position (where ionization occurs) for an ions whose orbit encloses the magnetic surface. This is the amount of radial displacement of the ion on which there is current.

we calculate the distances $\Delta^{t\pm}$, the times $t^{\pm}_{asymp}$ of this excursion and the drift velocities $v^{\pm}_{Di} = \Delta^{t\pm}/t^{\pm}_{asymp}$. This is shown in Figure 1 for ions with parallel, respectively anti-parallel initial velocity. The asymptotic position r_{asymp} is obtained by averaging a set of late values of $\overline{r}\,(t)$, for t beyond the vertical dashed lines. This ensures a good precision of identification of the "center". The straight line $r = r_{asymp}$ intersects the evolution line $\overline{r}\,(t)$ is a point marked by a open dot, the time t_{asymp}.

We have adopted a profile $S\,(r)$ which is constant in time, Figure 2. Its support is $[r_a, r_b]$ inside the interval $[r_1, r_2]$. The empty radial regions on both sides are necessary because the excursions of lengths $\Delta^{t\pm}$ of the ions generated at the ends of the support must be recorded in these regions. The result (the current $J\,(r,t)$) depends on time since the process that starts at $t = 0$ (no-ionization) rises slowly by accumulating current contributions, before saturation. More interesting is the spatial profile confirming that the sign of $\partial S/\partial r$ is decisive and that the total torque, *i.e.* integrated over the plasma volume, is zero, as expected from conservation of angular momentum and from the fact that no ion is lost from plasma in our picture. The current is plotted in Figure 3. In Figure 4 we show the mesh-cells that contribute to the current calculated in a reference cell, chosen arbitrarily in

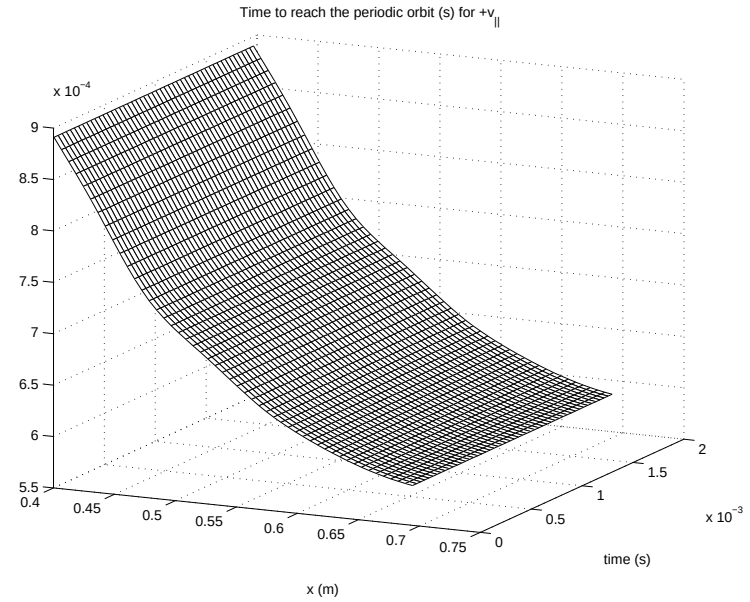

Figure 20: The (r, t) profile of the calculated time for an ion to reach the average position (the "center") starting from the place of ionization.

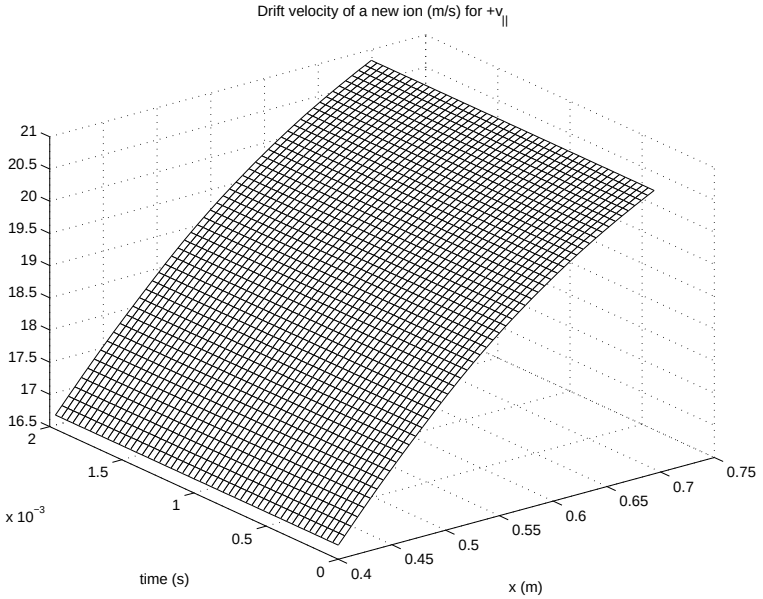

Figure 21: The (r, t) profile of the calculated drift velocity v_{Di}, as explained in Figure 7.

$(r, t) \equiv (ix = 350, itime = 150)$. The dots aligned on the a straight line (since v_{Di} =const) at left represent cells from where the new ions with positive (parallel) initial velocity arrive in r at t. The straight line at right represents ions with anti-parallel initial velocity.

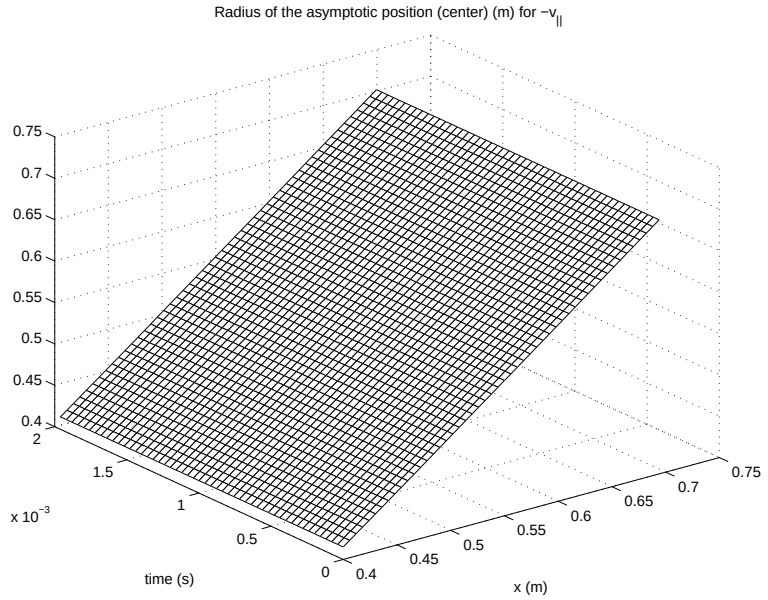

Figure 22: Same as Figure 18, but for ions whose orbits, calculated in every mesh-cell, are inside the magnetic surface.

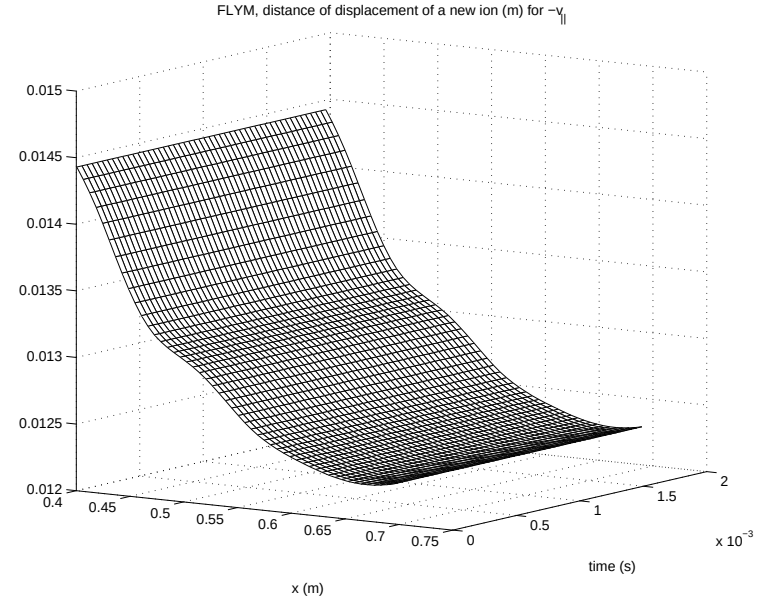

Figure 23: The variable $FLYM$, similar with $FLYP$ from Figure 19, but for the "smaller" banana.

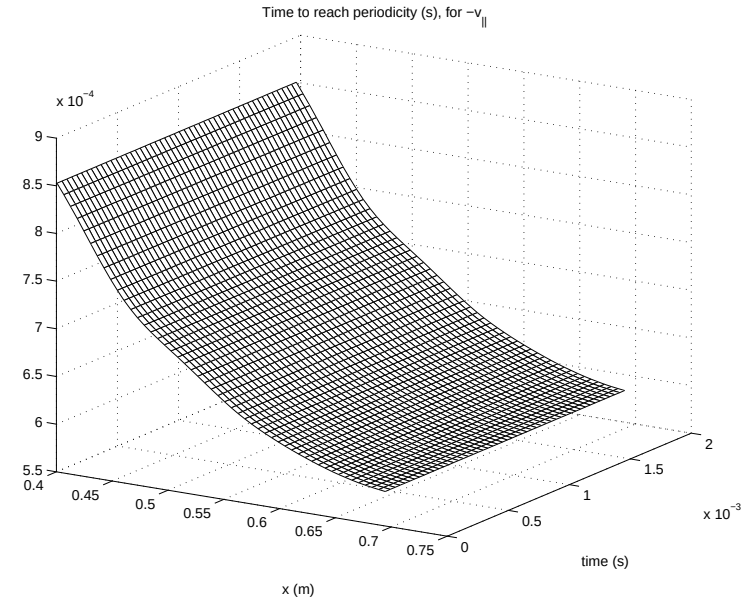

Figure 24: The time to reach the "center", for the "smaller" banana.

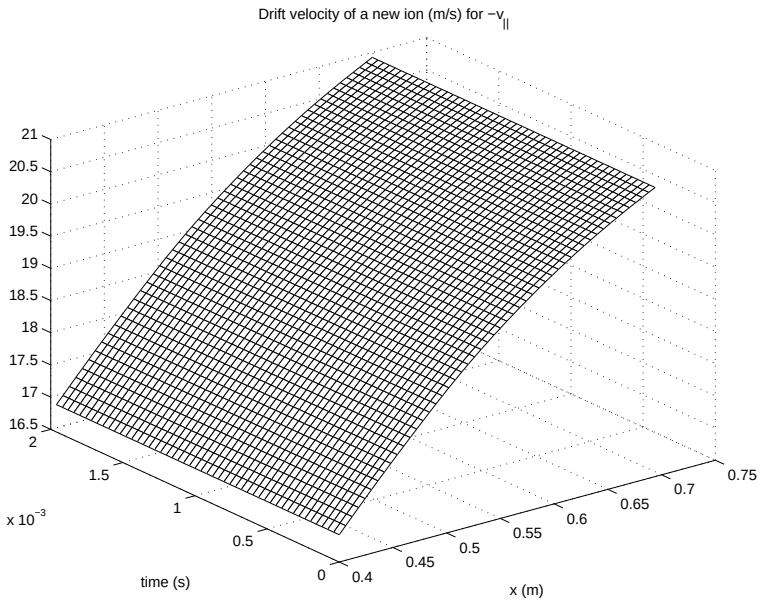

Figure 25: The drift velocity for the smaller banana.

IV. DRIFT-KINETIC CALCULATION OF THE IONIZATION-INDUCED CURRENT DENSITY

Similar problems are treated in the Ref.[11] (for alpha particles) and the Ref.[12] (for NBI). For the present case the drift-kinetic equation for the *new* ions, is

$$\frac{\partial f}{\partial t} + \left(v_{\|}\widehat{\mathbf{n}} + \mathbf{v}_{Di}\right) \cdot \nabla f = S^{ioniz} \tag{25}$$

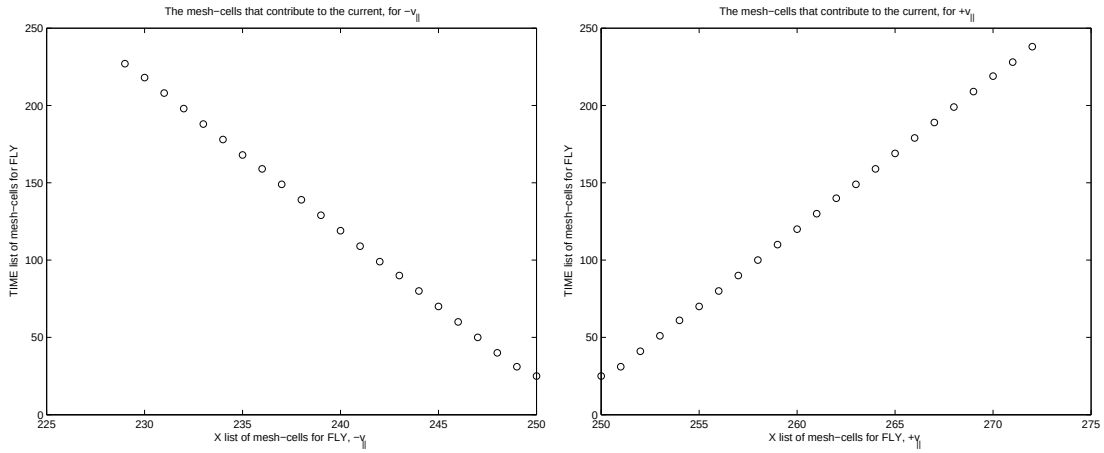

Figure 26: At left: the mesh-cells that are traversed by the ions generated in the point $(ir = 250, itime = 25)$ that evolve towards smaller radii (their banana orbits are fully inside the magnetic surface. At right: the mesh-cells that are traversed by the ions that evolve towards larger radii (their banana orbit ecloses the magnetic surface).

where the drift velocity of the guiding centre is $\mathbf{v}_{Di} = -v_{\parallel}\widehat{\mathbf{n}} \times \nabla \left(\frac{v_{\parallel}}{\Omega_{ci}}\right)$ and the neoclassical notations will be used: $\xi = v_{\parallel}/v = (1 - \lambda/h)^{1/2}$, $\lambda = hv_{\perp}^2/v^2$, $h = 1 + \varepsilon \cos\theta$. The *limits* of the trapped particle region in the variable λ are $1 - \frac{r}{R} < \lambda < 1 + \frac{r}{R}$. The velocity space variables are v, λ and σ (=sign of $v_{\parallel}$).

Since in this simple treatment we neglect the effect of collisions the neoclassical small parameter is the ratio of the banana half-width to the minor radius, $\delta = \Delta^{t\pm}/a \ll 1$. In usual neoclassical perturbative solution of the drift kinetic equation the zero order distribution function is the Maxwellian. In the present case, the perturbative expansion of f , the solution of the drift-kinetic equation for the new ions, must contain a term which is directly related to the source and, since this is determined by external factors, it cannot be ordered as powers of δ. The first term is formally of order -1, f_{-1}.

$$f = f_{-1} + f_0 + f_1 + ... \tag{26}$$

The lowest order

$$\widehat{\mathbf{n}} \cdot \nabla f_{-1} = 0 \tag{27}$$

shows that f_{-1} is constant along the magnetic lines, or $f_{-1} = f_{-1}(\psi)$. This result is connected with an assumption about the distribution of ionization processes in space: they have a rate which is constant on a magnetic surface.

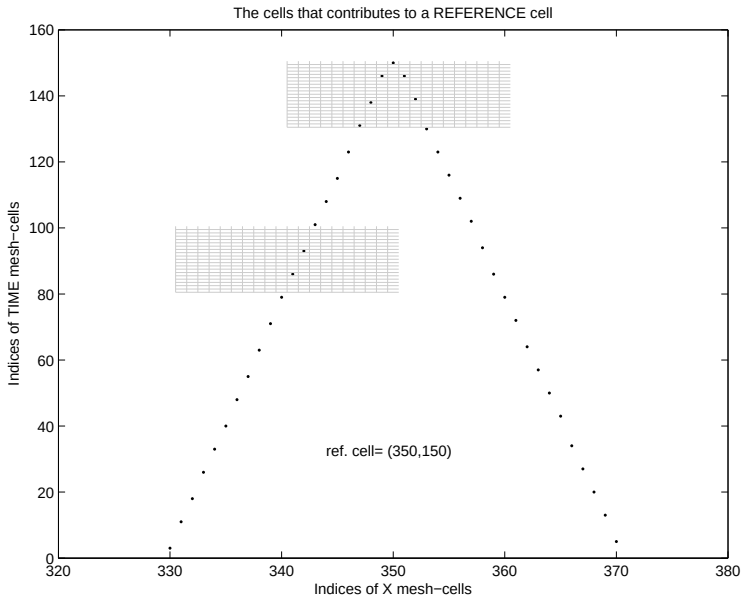

Figure 27: The mesh-cells that contribute to the current density that is "measured" in a reference cell (r,t), with indices of discretization $ir = 350$ and $itime = 150$. From the cells that are marked by a dot the ions are moving to larger radii (for the dots that are at the left of the axis of symmetry of the figure) and respectively to smaller radii (for the dots that are at the right of the axis of symmetry). Accordingly the contributions must have been generated by ionization in a position $r-\rho$ and respectively $r+\rho$, and at a time $t-\rho/v_{Di}$, for them to reach the reference cell at (r,t). The real mesh is too detailed to be shown and only two patches are shown, for illustration.

The zeroth order equation is

$$v_{\|}\widehat{\mathbf{n}}\cdot\nabla f_0 = -\mathbf{v}_{Di}\cdot\nabla\psi\frac{\partial f_{-1}}{\partial\psi} - \frac{\partial f_{-1}}{\partial t} + S^{ioniz} \tag{28}$$

As in any multiple space-time scale analysis we average at this level (0) to obtain a solution on the level (-1). We apply the operator of bounce averaging to eliminate the function f_0. This gives the equation

$$\frac{\partial f_{-1}}{\partial t} = \overline{S}^{ioniz} - \overline{\mathbf{v}_{Di}\cdot\nabla\psi}\frac{\partial f_{-1}}{\partial\psi} \tag{29}$$

The operator of *bounce averaging* is $\overline{A} = \frac{1}{T}\oint\frac{d\theta}{v_{\|}\widehat{\mathbf{n}}\cdot\nabla\theta}A = \frac{1}{T}\int\frac{d\theta}{v_{\|}/(qR)}A$. The bounce time is $T = \oint\frac{d\theta}{v_{\|}\widehat{\mathbf{n}}\cdot\nabla\theta} = \oint\frac{d\theta}{v_{\|}/(qR)}$. The limits of integrations for untrapped ions are $[-\pi\ ,\ \pi]$ and for trapped ions the integral is defined

$$\oint d\theta = \sum_{\sigma}\sigma\int_{-\theta_0}^{+\theta_0} d\theta \tag{30}$$

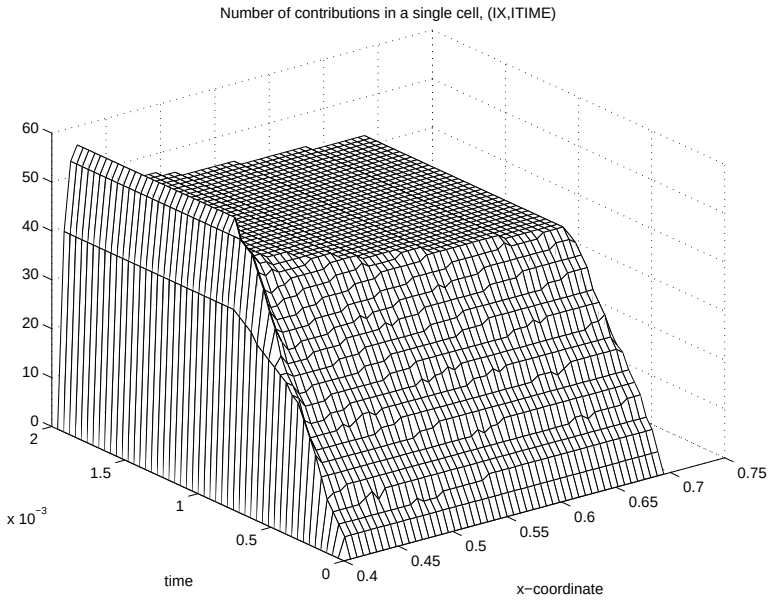

Figure 28: The (r,t) profile of the number of contributions that are registered in the cells of the mesh, coming from neighbor cells, as described in Figure 27.

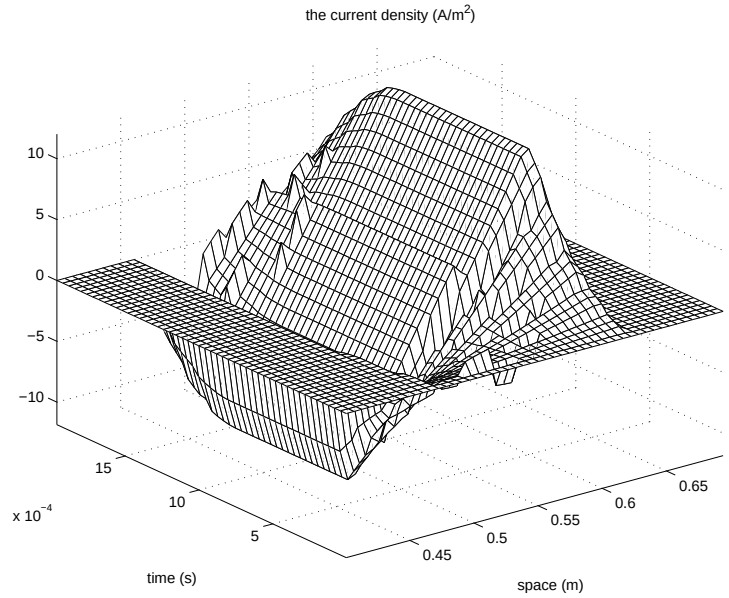

Figure 29: The (r,t) profile of the current density J $\left(A/m^2\right)$.

where $-\theta_0$ and $+\theta_0$ are the *turning points* of the banana. The radial projection of the guiding centre drift velocity can be written

$$\mathbf{v}_{Di} \cdot \nabla\psi = I v_{\parallel} \left(\widehat{\mathbf{n}} \cdot \nabla\right) \left(\frac{v_{\parallel}}{\Omega_{ci}}\right) = I v_{\parallel} \widehat{\mathbf{n}} \cdot \nabla\theta \frac{\partial}{\partial\theta} \left(\frac{v_{\parallel}}{\Omega_{ci}}\right) \tag{31}$$

where $I = R^2 \mathbf{B} \cdot \nabla\varphi = RB_T \equiv I\left(\psi\right)$ is a function of only the magnetic surface variable (ψ) and $\widehat{\mathbf{n}} \cdot \nabla\theta = 1/\left(qR\right)$. At this point we assume that the new ion has reached the asymptotic

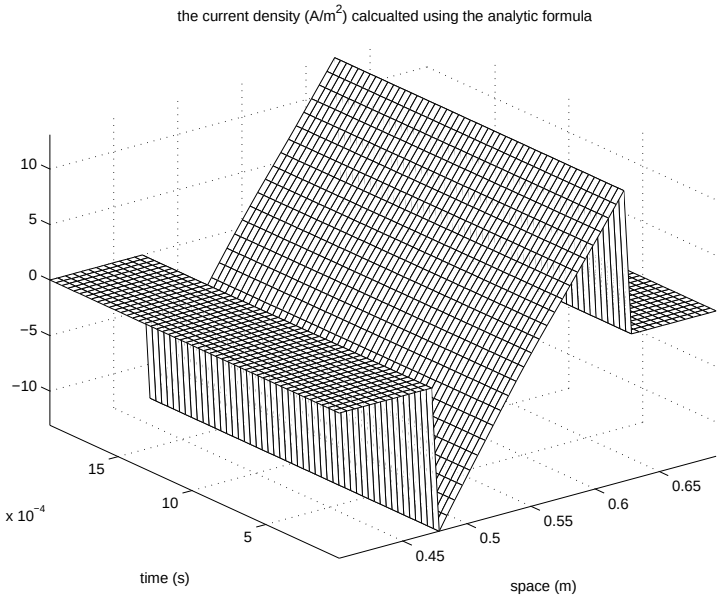

Figure 30: The first analytic formula that obtains the current density.

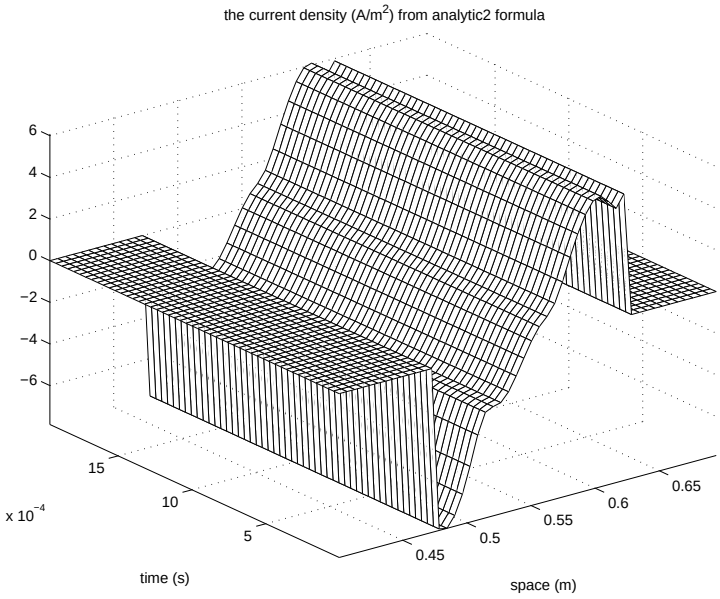

Figure 31: The second analytic formula for the current density.

periodic motion on the banana. Then the radial displacements average to zero

$$\overline{(\mathbf{v}_{Di} \cdot \nabla\psi)} = \frac{1}{T} \sum_{\sigma} \int_{-\theta_0}^{+\theta_0} \frac{d\theta}{v_{\parallel}/(qR)} I(\psi) \frac{v_{\parallel}}{qR} \frac{\partial}{\partial\theta} \left(\frac{v_{\parallel}}{\Omega_{ci}} \right) = 0 \tag{32}$$

Eq.(29) becomes

$$\frac{\partial f_{-1}}{\partial t} = \overline{S}^{ioniz} \tag{33}$$

and indeed f_{-1} appears as a direct result of the "external" source. The source of new ions

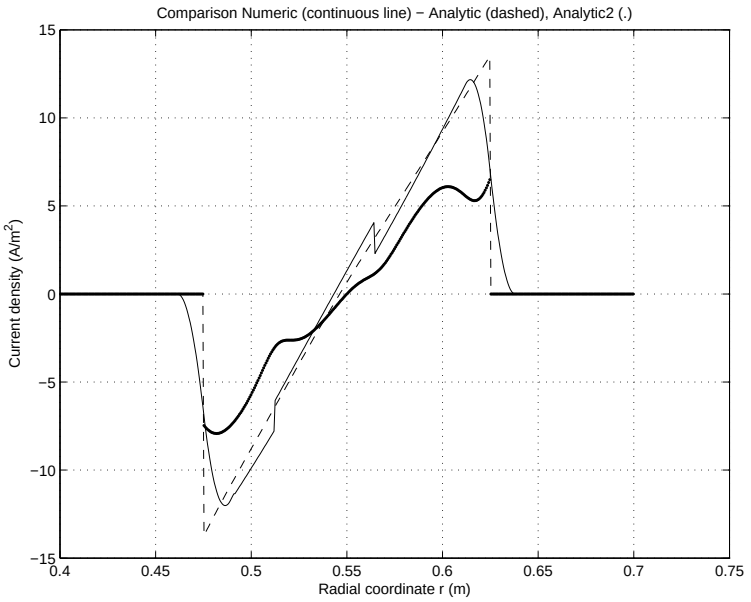

Figure 32: The comparison between the two analytic formulas and the result of the numerical calculation. The section is made at time that is half the total duration of the ionization process.

of velocity v_0, with direction σ_0 and trapping parameter λ_0 is[11]

$$\overline{S}^{ioniz} = \dot{n}^{ioniz}(\psi, t)\,\delta_{\sigma,\sigma_0}\Theta(t)\,\delta(\lambda - \lambda_0)\,\frac{\delta(v - v_0)}{\pi v_0^2} \tag{34}$$

The Eq.(33) simply describes the accumulation of new ions with $(v_0, \sigma_0, \lambda_0)$ on the surface ψ. The motion of these ions toward the banana trajectories and the periodic motion that follows must be found at higher orders. Returning to Eq.(28) we express f_0 in terms of f_{-1}, using (31)

$$v_\parallel \widehat{\mathbf{n}} \cdot \nabla f_0 \equiv v_\parallel \nabla_\parallel f_0 = -v_\parallel \nabla_\parallel \left(\frac{I v_\parallel}{\Omega_{ci}}\right) \frac{\partial f_{-1}(\psi)}{\partial \psi} \tag{35}$$

with the solution

$$f_0(\psi, \theta, t) = -I\left(\frac{v_\parallel}{\Omega_{ci}}\right) \frac{\partial f_{-1}(\psi)}{\partial \psi} + g(\psi, \theta, t) \tag{36}$$

where a constant of integration of the operator $\nabla_\parallel$ is introduced. We make few remarks. First, the time dependence of f_0 inherited from f_{-1} will be essential for the presence in the theory of the first, transitory and unique, part of the trajectory. Further, the first term can be approximated, using for circular geometry $\frac{I}{B_T}\frac{\partial}{\partial \psi} \simeq \frac{1}{B_\theta}\frac{\partial}{\partial r}$,

$$-I\left(\frac{v_\parallel}{\Omega_{ci}}\right) \frac{\partial f_{-1}(\psi)}{\partial \psi} \approx -\frac{B}{B_\theta}\frac{v_\parallel}{\Omega_{ci}}\frac{\partial f_{-1}(r)}{\partial r} = -\frac{v_\parallel}{\Omega_{\theta ci}}\frac{\partial}{\partial r} f_{-1}(r) \tag{37}$$

and we see that the difference between the distribution function f_0 and that of the previous level (f_{-1}) consists of a radial shift of the space argument, of the order of the poloidal

Larmor radius $v_\parallel/\Omega_{\theta ci} \sim \rho_\theta$. This is the same relationship as between the first order neoclassical distribution function relative to the Maxwellian equilibrium distribution[25]. In the particular case of trapped particles, the correction needs also to reflect the approximative relation between the thermal speed and the parallel velocity of ions[14], and we have $v_\parallel/\Omega_{\theta ci} \approx (v_{th}/\Omega_{\theta ci})\,(r/R)^{1/2} = \rho_\theta \varepsilon^{1/2}$. Finally we note that g is constant on the magnetic lines, *i.e.* on surfaces, $\widehat{\mathbf{n}} \cdot \nabla g = 0$. A distribution function for *bananas* can never be constant on the magnetic surfaces because the trajectory stops somewhere. Therefore g must only be added to (36) if we consider circulating particles. For our purpose it is not retained.

The next step is the equation for the *first order* f_1, which is derived from the equation written at *zero*-order

$$\frac{\partial f_0}{\partial t} + v_\parallel \widehat{\mathbf{n}} \cdot \nabla f_1 + \mathbf{v}_{Di} \cdot \nabla f_0 = 0 \tag{38}$$

This involves the variation of the first order correction function f_1 along the magnetic lines $v_\parallel \nabla_\parallel f_1 + ...$

$$\mathbf{v}_{Di} \cdot \nabla f_0 = \mathbf{v}_{Di} \cdot \nabla\theta \frac{\partial f_0}{\partial \theta} + \mathbf{v}_{Di} \cdot \nabla\psi \frac{\partial f_0}{\partial \psi} \tag{39}$$

where $\mathbf{v}_{Di} = -v_\parallel \widehat{\mathbf{n}} \times \nabla \left(\frac{v_\parallel}{\Omega_{ci}}\right)$.

$$\mathbf{v}_{Di} \cdot \nabla\theta = v_\parallel \frac{1}{r} R B_\theta \frac{\partial}{\partial \psi}\left(\frac{v_\parallel}{\Omega_{ci}}\right) \tag{40}$$

and similarly

$$\mathbf{v}_{Di} \cdot \nabla\psi = -\frac{v_\parallel}{r} R B_\theta \frac{\partial}{\partial \theta}\left(\frac{v_\parallel}{\Omega_{ci}}\right) \tag{41}$$

Returning to the initial expression

$$\mathbf{v}_{Di} \cdot \nabla f_0 = I \frac{v_\parallel}{qR}\left[\frac{\partial}{\partial \psi}\left(\frac{v_\parallel}{\Omega_{ci}}\right)\frac{\partial f_0}{\partial \theta} - \frac{\partial}{\partial \theta}\left(\frac{v_\parallel}{\Omega_{ci}}\right)\frac{\partial f_0}{\partial \psi}\right] \tag{42}$$

The *bounce average* is

$$\overline{(\mathbf{v}_{Di} \cdot \nabla f_0)} = \frac{1}{T} I \int_{-\theta_0}^{+\theta_0} \frac{d\theta}{v_\parallel/(qR)} \frac{v_\parallel}{qR}\left[\frac{\partial}{\partial \psi}\left(\frac{v_\parallel}{\Omega_{ci}}\right)\frac{\partial f_0}{\partial \theta} - \frac{\partial}{\partial \theta}\left(\frac{v_\parallel}{\Omega_{ci}}\right)\frac{\partial f_0}{\partial \psi}\right] \tag{43}$$

Here we replace f_0 with its expression in terms of f_{-1};

$$f_0(\psi, \theta, t) = -I\left(\frac{v_\parallel}{\Omega_{ci}}\right)\frac{\partial f_{-1}(\psi)}{\partial \psi} \tag{44}$$

$$\overline{(\mathbf{v}_{Di}\cdot\nabla f_0)} \tag{45}$$
$$= -\frac{I^2}{T}\int_{-\theta_0}^{+\theta_0} d\theta \left\{ \frac{\partial}{\partial\psi}\left(\frac{v_\parallel}{\Omega_{ci}}\right)\frac{\partial}{\partial\theta}\left(\frac{v_\parallel}{\Omega_{ci}}\right)\frac{\partial f_{-1}(\psi)}{\partial\psi} + \frac{\partial}{\partial\psi}\left(\frac{v_\parallel}{\Omega_{ci}}\right)\left(\frac{v_\parallel}{\Omega_{ci}}\right)\frac{\partial^2 f_{-1}(\psi)}{\partial\theta\partial\psi} \right.$$
$$\left. -\frac{\partial}{\partial\theta}\left(\frac{v_\parallel}{\Omega_{ci}}\right)\frac{\partial}{\partial\psi}\left(\frac{v_\parallel}{\Omega_{ci}}\right)\frac{\partial f_{-1}(\psi)}{\partial\psi} - \frac{\partial}{\partial\theta}\left(\frac{v_\parallel}{\Omega_{ci}}\right)\left(\frac{v_\parallel}{\Omega_{ci}}\right)\frac{\partial^2 f_{-1}}{\partial\psi^2}\right\}$$

The first and third terms cancel. In addition we know from (27) that f_{-1} is constant on the magnetic surfaces. *i.e.* the second term is zero. It remains

$$\overline{(\mathbf{v}_{Di}\cdot\nabla f_0)} = \frac{I^2}{T}\frac{\partial^2 f_{-1}}{\partial\psi^2}\int_{-\theta_0}^{+\theta_0} d\theta \frac{\partial}{\partial\theta}\left[\frac{1}{2}\left(\frac{v_\parallel}{\Omega_{ci}}\right)^2\right] = 0 \tag{46}$$

We can now calculate the radial current, using the distribution functions in orders -1, 0, 1. This is obtained from the radial projection of the drift velocity, Eq.(31)

$$\mathbf{v}_{Di}\cdot\nabla\psi = I\frac{v_\parallel}{qR}\frac{\partial}{\partial\theta}\left(\frac{v_\parallel}{\Omega_{ci}}\right) \tag{47}$$

The current is projected on the radial direction and the result is averaged over the magnetic surface, with the operator $\langle A\rangle = w^{-1}\int Ard\theta/B_\theta$, $w = \int rd\theta/B_\theta$,

$$\langle \mathbf{j}\cdot\nabla\psi\rangle = |e|\left\langle \int d^3v\,(\mathbf{v}_{Di}\cdot\nabla\psi)\,f\right\rangle = -|e|\,I\left\langle\int d^3v\left(\frac{v_\parallel}{\Omega_{ci}}\right)v_\parallel\widehat{\mathbf{n}}\cdot\nabla f\right\rangle \tag{48}$$

An integration by parts over θ has been done. Two terms are absent: (1) the order -1 distribution function f_{-1} does not contribute due to (27); and (2) the order 0 does not contribute, due to (46). The first order to have a contribution to this current (averaged over surface) is f_1. From the equation (38) we take the term

$$v_\parallel\widehat{\mathbf{n}}\cdot\nabla f_1 = -\frac{\partial f_0}{\partial t} - \mathbf{v}_{Di}\cdot\nabla f_0 \tag{49}$$

and Eq.(48) becomes

$$\langle \mathbf{j}\cdot\nabla\psi\rangle = -|e|\,I\left\langle\int d^3v\left(\frac{v_\parallel}{\Omega_{ci}}\right)\left(-\frac{\partial f_0}{\partial t} - \mathbf{v}_{Di}\cdot\nabla f_0\right)\right\rangle \tag{50}$$

The surface average operator applied on the second term in the bracket vanishes

$$\left\langle\int d^3v\left(\frac{v_\parallel}{\Omega_{ci}}\right)(\mathbf{v}_{Di}\cdot\nabla f_0)\right\rangle = 0 \tag{51}$$

This is shown by a calculation analogous to that of Eq.(39), using (40) and (41) followed by the substitution of (44). The current is

$$\langle \mathbf{j}\cdot\nabla\psi\rangle = |e|\,I\left\langle\int d^3v\left(\frac{v_\parallel}{\Omega_{ci}}\right)\frac{\partial f_0}{\partial t}\right\rangle \tag{52}$$

We use the zero-order function f_0 from Eq.(44) and take the time derivative,

$$\langle \mathbf{j} \cdot \nabla \psi \rangle = - |e| I^2 \left\langle \int d^3v \left(\frac{v_\parallel}{\Omega_{ci}} \right)^2 \frac{\partial^2 f_{-1}}{\partial \psi \partial t} \right\rangle \tag{53}$$

where, in (34) we keep the isotropic velocity space integration $d^3v = 4\pi v^2 dv$ and introduce the factorization (2)

$$\frac{\partial f_{-1}}{\partial t} = \overline{S}^{ioniz} = \overset{.}{n}_0^{ioniz} S(r,t) \frac{1}{4\pi v^2} \delta(v - v_0) \tag{54}$$

For circular surfaces

$$\langle j_r \rangle \approx - |e| \frac{B_T^2}{B_\theta^2} \left\langle \int d^3v \left(\frac{v_\parallel}{\Omega_{ci}} \right)^2 \frac{\partial^2 f_{-1}}{\partial r \partial t} \right\rangle \tag{55}$$

We note again the presence of the poloidal gyroradius, corrected for trapped particles ($v_\parallel = (r/R)^{1/2} v_{th}$),

$$\frac{B_T^2}{B_\theta^2} \left(\frac{v_\parallel}{\Omega_{ci}} \right)^2 \approx \left(\frac{v_\parallel}{\Omega_{\theta ci}} \right)^2 = \rho_\theta^2 \varepsilon = \rho_i^2 q^2 \varepsilon^{-1} \tag{56}$$

This length $\left(\rho_\theta \varepsilon^{1/2}\right)$ corresponds to the radial excursion of the new ion, as defined in our previous approach, Eq.(21)

$$\rho_\theta \varepsilon^{1/2} = \rho_i q \varepsilon^{-1/2} \approx \Delta^{t\pm} \tag{57}$$

After replacing the expression of $\partial f_{-1}/\partial t$ Eq.(54) we have

$$\begin{aligned} \langle j_r \rangle &= - |e| \left\langle \int d^3v \rho_\theta^2 \varepsilon \frac{\partial}{\partial r} \overset{.}{n}_0^{ioniz} S(r,t) \frac{1}{4\pi v^2} \delta(v - v_0) \right\rangle \\ &= - |e| \overset{.}{n}_0^{ioniz} \frac{\partial S(r,t)}{\partial r} \left\langle \rho_\theta^2 \varepsilon \right\rangle = - |e| \overset{.}{n}_0^{ioniz} \frac{\partial S(r,t)}{\partial r} \left\langle \left(\Delta^{t\pm} \right)^2 \right\rangle \end{aligned} \tag{58}$$

It is understood that ρ_θ and further $\Delta^{t\pm} = \rho_i q \varepsilon^{-1/2}$ are calculated at the velocity v_0. As before we replace the λ-integration with multiplication with $\sqrt{\varepsilon}$, fraction of trapped particles

$$j_r = -\gamma |e| \overset{.}{n}_0^{ioniz} \frac{\partial S(r,t)}{\partial r} \rho_i^2 q^2 \varepsilon^{-1/2} \tag{59}$$

The constant γ is a purely neoclassical constant and is calculated, for more general conditions, in[11]. It includes the exact integration over the trapping parameter λ, which is contained in $v_\parallel$ at v_0 fixed. The result is $\gamma \sim 0.38$.

We note that the analytic structure of our result Eq.(22) and of its rederivation in the neoclassical drift-kinetic theory, Eq.(59) are the same as the expression obtained in the treatment of Rosenbluth and Hinton for the current induced by the α particles[11]. The coefficient in our approximate treatment Eq.(22) is $\gamma \sim 1/2$. Figure 5 represents the space

dependence of the current $J(r, t_0)$ obtained from the analysis of the physical picture, Eq.(20), from the numerical model and respectively from Eq.(22) which is also the result of the drift-kinetic approach. The time t_0 is chosen at half the total time interval, to avoid the transient after the onset of ionization.

We note that the conclusion of the mentioned paper, that the rotation induced by the creation of *alpha* particles is insignificant is a consequence of the very small nuclear reaction rate. The equivalent parameter, in the present problem, is the rate of generation of new ions, which is three orders of magnitude higher in the case of pellets.

The two treatments (the simple arguments related with the fluxes of ions and, respectively, the drift-kinetic equation) lead to the same result but there is an apparent difference between them. In the first treatment the separation of the trajectory of a new ion in a transitory part, where effective current exist, and a periodic part with no effective radial current is the key element that identifies the source of current, torque, rotation. In the drift-kinetic approach this separation is not obvious. One would expect an "initial value problem" where the distribution function would result as integral over the history of the ion's motion. This is not visible. The Heaviside function of the source is not helpful either: it marks the beginning of the ionization process but after that every moment of time is a source of new ions and this is not represented. We understand however that the separation is implicitly done through the velocity space integration. The current is defined as $j \sim |e| \left\langle v_{Di} \int d^3v \overline{f}(r, v) \right\rangle$. The late phase of the ion orbit is periodic and the integral mixes to zero the two-way travels on banana, leaving only the first, non-periodic, part.

V. DISCUSSION AND CONCLUSION

The gas puff, the pellets, the impurity seeding and in general any inflow of neutrals into plasma produce a substantial radial current and implicitly a torque that can be higher than the magnetic pumping damping. It can be shown that it can also be higher than the turbulent Reynolds stress and the Stringer mechanism. We have derived a simple analytical expression which is confirmed by numerical simulation. Furthermore, we have re-derived it within the neoclassical drift-kinetic approach. All three methods have close quantitative results, as shown in Figure 5. We mention, qualitatively, few possible consequences.

PEP regimes[1] seem to be connected with the ionization-induced rotation that improves

the local confinement by creating effective barriers through the sheared poloidal flow[5]. The duration of the PEP and the density peaking are compatible with ionization-induced rotation.

The ionization-induced radial current leads to density peaking, in at least three different ways. If the gradient of the rate of ionization of a pellet is negative ($\partial S/\partial r < 0$, higher ionization rate close to the plasma center, as for pellets launched from high-field side) then the current Eq.(22) is directed toward the edge. The bulk ions must move toward the magnetic axis to compensate this current. Schematically, we consider a new ion that moves a distance Δ toward the edge and then "stops" (actually it moves periodically on banana). An ion of the background must move in opposite direction the same distance Δ. But in that moment another new ion is created at a distance Δ from this position, closer to the center and starts moving toward the edge. Then the background ion must continue its displacement toward the center to compensate this new current. While any new ion move a distance Δ then stops, the background ion must continue to move to compensate the small currents. Quantitatively the two fluxes are balanced but ions from edge can travel very far toward the center. Impurity accumulation in the center can also be produced in this process.

Second, the rotation produced at ionization is necessarily sheared, *i.e.* $v_\theta = v_\theta(r)$, for two reasons. In the regions of positive and respectively negative radial derivative of the rate of ionization ($\partial S/\partial r \gtrless 0$) the rotation has opposite direction (Figures 3 and 5). In addition, the background ions must have a local rotation that is opposite to that of the new ions. The rate of extraction of the free energy from density gradients is reduced and the turbulence will have shorter radial correlation length. The rate of transport decreases and the peaking of the density in the center is enhanced by the smaller density diffusion.

Third, the shear of the poloidal velocity is actually vorticity $\omega = \partial v_\theta/\partial r$ and when this occurs the Ertel's theorem $\frac{d}{dt}\left(\frac{\omega+\Omega_{ci}}{n}\right) = 0$ imposes a redistribution of density.

A change of the density at the edge, by impurity seeding[3] or by other strong ionization event, must now also be regarded as an electric process, due to the charge separation and the radial current of the new ions. It implies that very fast plasma responses should be expected[26]. This may explain observed fast propagation of perturbations, sometimes called "non-local". Fast increase of the radial electric field is able to determine, as a neoclassical effect, the reversal of the toroidal rotation[27],[28],[29].

In conclusion, we have presented arguments that the neoclassical displacements of the new ions generated at ionization (of gas puff, pellet, impurity seeding) produce a radial current that can be substantial. The current is generated from the first part, transitory, unique for any ionization event, of the trajectory: between the ionization and the moment where the new ion reaches the stationary periodic motion, trapped or circulating. The torque resulting from ionization can be substantial and it can generate internal transport barriers. Our perspective on some particular regimes may need reconsideration: Pellet Enhanced Performance, density peaking, density pinch, regimes with density higher than the Greenwald limit, fast propagation of edge effects, influence of the density on the transition to H-mode, connection between density and rotation, reversal of toroidal rotation, etc. A more detailed investigation of the ionization-induced rotation is requested, for each of these cases.

VI. APPENDIX. COMPARISON OF THE CURRENTS CARRIED BY TRAPPED AND RESPECTIVELY CIRCULATING IONS

The equation of the closed orbit (poloidal projection of the orbit of a circulating ion) is

$$(x+\alpha r_0)^2 + y^2 = r_0^2 \tag{A.1}$$

a circle of radius r_0 that is displaced from the magnetic axis with the amount $x_0 = \alpha r_0$ where $\alpha = (B/B_T)\, v_{Di}/v_\parallel$ =const.[21]. We have $\alpha \ll 1$ (since $v_{Di} \ll v_\parallel \sim v_{th,i}$) for circulating ions. Therefore the radial displacement of the "center" of the orbit of a new ion that is circulating, relative to the center of the magnetic surface where it is created, is small. The displacement x_0 of circulating ions that are created closer to the edge (at higher r_0) are larger than that created closer to the magnetic axis. For two ions born in the same point on the equatorial plane and with velocities parallel respectively anti-parallel to $\mathbf{B}$ the difference between these displacements is linear in r,

$$\begin{aligned} \left| x_0^{(+)} - x_0^{(-)} \right| &= \left| \left(x_{0c} + \alpha \frac{\partial r_0}{\partial r} x_0^{(+)} \right) - \left(x_{0c} - \alpha \frac{\partial r_0}{\partial r} x_0^{(-)} \right) \right| \\ &= \alpha \frac{\partial r_0}{\partial r} \left(x_0^{(+)} + x_0^{(-)} \right) = 2\alpha^2 r_0 \end{aligned} \tag{A.2}$$

This is indeed very small, due to α^2 factor. The closed orbit for parallel initial velocity, (+), is fully contained inside the magnetic surface, which means that the displacement $x_0^{(+)}$

is positive. The closed orbit for the anti-parallel initial velocity, $(-)$, fully encloses the magnetic surface, which means that the displacement $x_0^{(-)}$ is negative. In absolute value $x_0^{(+)}$ is greater than $x_0^{(-)}$. Note that we here use the geometric "center of the closed orbit" and *not* the asymptotic value of the average $\overline{x}\,(t \to \infty)$. The latter are closer the main axis of symmetry, for both sign of the initial velocities.

The current carried by the new ions for the short time until they access the stationary periodic motion relies on the difference between the displacements $n^c \left| x_0^{(+)} - x_0^{(-)} \right| = n^c 2\alpha^2 r$ is directed towards the main axis of the torus. The ratio between the width of the banana and the displacement of the center for a circulating particle originating from the same point is approximately[21]

$$\frac{\Delta^{\pm}}{x_0^{(\pm)}} = 4\sqrt{\frac{R_0}{r}} \tag{A.3}$$

The second term in Eq.(20) is in general greater than the first. We then compare the current from circulating ions with only this first term. We find that the circulating ions' contribution is smaller than this term, which justifies their neglect adopted in the main text. We have to compare the charge displacements, including the densities of trapped (n^t) and circulating (n^c) particles. We expand, taking as reference position the point r where the two ions (with parallel and anti-parallel $\mathbf{v}_0$) are born, $\Delta^{(+)} - \Delta^{(-)} = \frac{\partial \Delta}{\partial r}\left[\Delta^{(+)} + \Delta^{(-)}\right]$. In the right hand side, and in all expressions where the difference between $\Delta^{\pm}$ is not involved, we can approximate $\Delta = \Delta^{\pm}(r) \approx \rho_i q\,(r)\,\varepsilon^{-1/2}/2$.

$$\frac{n^t \left|\Delta^{(+)} - \Delta^{(-)}\right|}{n^c \left| x_0^{(+)} - x_0^{(-)} \right|} \approx \frac{\frac{1}{2} n^t \frac{(\rho_i q)^2}{\varepsilon} \frac{\partial}{\partial r} \ln\left(q r^{-1/2}\right)}{2 n^c \alpha^2 r} \tag{A.4}$$

We use $\partial\varepsilon/\partial r \approx 1/R$ and $(\rho_i q) = 2\Delta\sqrt{\varepsilon}$ obtaining the ratio

$$\frac{1}{\alpha^2 r^2} R\,(\rho_i q)^2 = r\left(\frac{\Delta}{x_0}\right)^2 \tag{A.5}$$

Then

$$\frac{n_i^t \left|\Delta^{(+)} - \Delta^{(-)}\right|}{n_i^c \left| x_0^{(+)} - x_0^{(-)} \right|} = \frac{n_i^t}{n_i^c} r \left(\frac{\Delta}{x_0}\right)^2 \frac{1}{4} \frac{\partial}{\partial r} \ln\left(q r^{-1/2}\right) \tag{A.6}$$

The ratio of the densities of trapped and circulating particles is

$$\frac{n_i^t}{n_i^c} \approx \frac{\sqrt{\varepsilon}}{1 - \sqrt{\varepsilon}} \tag{A.7}$$

and employing Eq.(A.3)

Then

$$\frac{n^t\left|\Delta^{(+)}-\Delta^{(-)}\right|}{n^c\left|x_0^{(+)}-x_0^{(-)}\right|}\approx 4R_0\frac{\sqrt{\varepsilon}}{1-\sqrt{\varepsilon}}\frac{\partial}{\partial r}\ln\left(qr^{-1/2}\right) \tag{A.8}$$

In the region of interest $[r_1, r_2]$ it is sufficient to approximate $q \sim 1+\beta\left(r/a\right)^2$ with β a constant. Retaining the dominant term, $\frac{\partial}{\partial r}\ln\left(qr^{-1/2}\right) \sim \frac{3}{2}\frac{1}{r}$ we have the estimation

$$\frac{n^t\left|\Delta^{(+)}-\Delta^{(-)}\right|}{n^c\left|x_0^{(+)}-x_0^{(-)}\right|}\approx \frac{6}{\sqrt{\varepsilon}-\varepsilon}\gg 1 \tag{A.9}$$

This justifies the neglect of the current from the circulating ions in Eqs.(19) and (20).

REFERENCES

[1]P. Smeulders, L. Appel, B. Balet, T. Hender, L. Lauro-Taroni, D. Stork, B. Wolle, S. Ali-Arshad, B. Alper, H. D. Blank, M. Bures, B. D. Esch, R. Giannella, R. Konig, P. Kupschus, K. Lawson, F. Marcus, M. Mattioli, H. Morsi, D. O'Brien, J. O'Rourke, G. Sadler, G. Schmidt, P. Stubberfield, and W. Zwingmann, "Survey of pellet enhanced performance in jet discharges," Nuclear Fusion **35**, 225 (1995).

[2]M. Hugon, B. van Milligen, P. Smeulders, L. Appel, D. Bartlett, D. Boucher, A. Edwards, L.-G. Eriksson, C. Gowers, T. Hender, G. Huysmans, J. Jacquinot, P. Kupschus, L. Porte, P. Rebut, D. Start, F. Tibone, B. Tubbing, M. Watkins, and W. Zwingmann, "Shear reversal and mhd activity during pellet enhanced performance pulses in jet," Nuclear Fusion **32**, 33 (1992).

[3]G. Jackson, M. Murakami, G. McKee, D. Baker, J. Boedo, R. L. Haye, C. Lasnier, A. Leonard, A. Messiaen, J. Ongena, G. Staebler, B. Unterberg, M. Wade, J. Watkins, and W. West, "Effects of impurity seeding in diii-d radiating mantle discharges," Nuclear Fusion **42**, 28 (2002).

[4]L. R. Baylor, T. C. Jernigan, S. K. Combs, W. A. Houlberg, M. Murakami, P. Gohil, K. H. Burrell, C. M. Greenfield, R. J. Groebner, C.-L. Hsieh, R. J. L. Haye, P. B. Parks, G. M. Staebler, D.-D. Team, G. L. Schmidt, D. R. Ernst, E. J. Synakowski, and M. Porkolab, "Improved core fueling with high field side pellet injection in the diii-d tokamak," Phys. Plasmas **7**, 1878–1885 (2000).

[5]C. L. Fiore, D. R. Ernst, J. E. Rice, K. Zhurovich, N. Basse, P. T. Bonoli, M. J. Greenwald, E. S. Marmar, and S. J. Wukitch, "Internal transport barriers in alcator c-mod," Fusion Science and Technology **51**, 303–316 (2007).

[6]M. Valovic, L. Garzotti, C. Gurl, R. Akers, J. Harrison, C. Michael, G. Naylor, R. Scannell, and the MAST team, "H-mode access by pellet fuelling in the mast tokamak," Nuclear Fusion **52**, 114022 (2012).

[7]W. Liu and M. Talvard, "Rapid global response of the electron temperature during pellet injection on tore supra," Nuclear Fusion **34**, 337 (1994).

[8]M. Tournianski, P. Carolan, N. Conway, G. Counsell, A. Field, and M. Walsh, "Poloidal rotation and associated edge behaviour in start plasmas," Nuclear Fusion **41**, 77 (2001).

[9]F. Spineanu and M. Vlad, "The role of the rotation in the correlated transient change of the density and confinement," (40^{th} EPS Conference on Plasma Physics, 2013) helsinki, Finland, 1-5 July 2013. Paper P1.178.

[10]J. Nycander and V. Yankov, "H-mode in tokamaks attributed to absence of trapped ions in poloidally rotating plasma," Pisma Zh. Eksp. Teor. Fiz. **63**, 427–430 (1996).

[11]M. Rosenbluth and F. Hinton, "Plasma rotation driven by alpha particles in a tokamak reactor," Nucl. Fusion **36**, 55–67 (1996).

[12]F. Hinton and M. Rosenbluth, "The mechanism for the toroidal momentum input to tokamak plasma from neutral beams," Phys. Letters **A259**, 267–275 (1999).

[13]B. Fong and T. Hahm, "Bounce averaged kinetic equations and neoclassical polarization density," Physics of Plasmas **6**, 189–199 (1999).

[14]M. N. Rosenbluth, R. D. Hazeltine, and F. L. Hinton, "Plasma transport in toroidal confinement systems," Physics of Fluids (1958-1988) **15**, 116–140 (1972).

[15]P. T. Lang, B. Alper, L. R. Baylor, M. Beurskens, J. G. Cordey, R. Dux, R. Felton, L. Garzotti, G. Haas, L. D. Horton, S. Jachmich, T. T. C. Jones, A. Lorenz, P. J. Lomas, M. Maraschek, H. W. Mller, J. Ongena, J. Rapp, K. F. Renk, M. Reich, R. Sartori, G. Schmidt, M. Stamp, W. Suttrop, E. Villedieu, D. Wilson, and E.-J. workprogramme collaborators, "High density operation at jet by pellet refuelling," Plasma Physics and Controlled Fusion **44**, 1919 (2002).

[16]W. Houlberg, S. Attenberger, L. Baylor, M. Gadeberg, T. Jernigan, P. Kuschus, S. Milora, G. Schmidt, D. Swain, and M. Watkins, "Pellet penetration experiments on jet," Nucl. Fusion **32**, 1951–1965 (1992).

[17]L. Baylor, G. Schmidt, W. Houlberg, S. Milora, C. Gowers, W. Bailey, M. Gadeberg, P. Kupschus, J. Tagle, D. Owens, D. Mansfield, and H. Park, "Pellet fuelling deposition measurements on jet and tftr," Nuclear Fusion **32**, 2177 (1992).

[18]L. Baylor, T. Jernigan, P. Parks, G. Antar, N. Brooks, S. Combs, D. Fehling, C. Foust, W. Houlberg, and G. Schmidt, "Comparison of deuterium pellet injection from different locations on the diii-d tokamak," Nuclear Fusion **47**, 1598 (2007).

[19]A. B. Hassam and R. M. Kulsrud, "Time evolution of mass flows in a collisional tokamak," Physics of Fluids (1958-1988) **21**, 2271–2279 (1978).

[20]R. E. Bell, F. M. Levinton, S. H. Batha, E. J. Synakowski, and M. C. Zarnstorff, "Core poloidal rotation and internal transport barrier formation in tftr," Plasma Physics and Controlled Fusion **40**, 609 (1998).

[21]A. Morozov and L. Solovev, "Motion of charged particles in electro-magnetic fields," in *Reviews of Plasma Physics*, Vol. 2, edited by M. Leontovich (Consultants Bureau, New York, 1966) pp. 201–297.

[22]H. Berk and A. Galeev, "Velocity space instabilities in a toroidal geometry," Phys. Fluids **10**, 441–450 (1967).

[23]A. Galeev and R. Sagdeev, "Theory of neoclassical diffusion," in *Reviews of Plasma Physics*, Vol. 7, edited by M. Leontovich (Consultants Bureau, New York, 1979) pp. 257–343.

[24]S. Wong and K. Burrell, "Transport theory of tokamak plasmas with large toroidal rotation," Phys. Fluids **25**, 1863–1870 (1982).

[25]F. Hinton and R. Hazeltine, "Theory of plasma transport in toroidal confinement systems," Rev. Mod. Phys. **48**, 239–308 (1976).

[26]F. Spineanu and M. Vlad, "Fluctuation of the ambipolar equilibrium in magnetic perturbations," Physics of Plasmas **9**, 5125–5128 (2002).

[27]J. Rice, B. Duval, M. Reinke, Y. Podpaly, A. Bortolon, R. Churchill, I. Cziegler, P. Diamond, A. Dominguez, P. Ennever, C. Fiore, R. Granetz, M. Greenwald, A. Hubbard, J. Hughes, J. Irby, Y. Ma, E. Marmar, R. McDermott, M. Porkolab, N. Tsujii, and S. Wolfe, "Observations of core toroidal rotation reversals in alcator c-mod ohmic l-mode plasmas," Nuclear Fusion **51**, 083005 (2011).

[28]J. E. Rice, W. D. Lee, E. S. Marmar, N. P. Basse, P. T. Bonoli, M. J. Greenwald, A. E. Hubbard, J. W. Hughes, I. H. Hutchinson, A. Ince-Cushman, J. H. Irby, Y. Lin, D. Mosses-

sian, J. A. Snipes, S. M. Wolfe, S. J. Wukitch, and K. Zhurovich, "Toroidal rotation and momentum transport in alcator c-mod plasmas with no momentum input," Physics of Plasmas (1994-present) **11**, 2427–2432 (2004).

[29]F. Spineanu and M. Vlad, "A model for the reversal of the toroidal rotation in tokamak," Nuclear Fusion **52**, 114019 (2012).